THE JOURNAL OF GENE MEDICINE
J Gene Med 2005; 7: 108–116.
Published online 27 October 2004 in Wiley InterScience (www.interscience.wiley.com). DOI: 10.1002/jgm.632

RESEARCH ARTICLE

An efficient gene transfer method mediated by ultrasound and microbubbles into the kidney

Hiromi Koike[1]
Naruya Tomita[1,2]*
Haruhito Azuma[3]
Yoshiaki Taniyama[1,2]
Keita Yamasaki[1]
Yasuo Kunugiza[1]
Katsuro Tachibana[4]
Toshio Ogihara[2]
Ryuichi Morishita[1]

[1]*Division of Clinical Gene Therapy, Osaka University Graduate School of Medicine, Suita 565-0871, Japan*

[2]*Department of Geriatric Medicine, Osaka University Graduate School of Medicine, Suita 565-0871, Japan*

[3]*Department of Urology, Osaka Medical College, Takatsuki 569-8686, Japan*

[4]*Department of Anatomy, Fukuoka University School of Medicine, Fukuoka 814-0180, Japan*

*Correspondence to:
Naruya Tomita, Division of Clinical Gene Therapy, Osaka University Graduate School of Medicine, 2-2 Yamada-oka, Suita 565-0871, Japan. E-mail: tomita@hp-gm.med.osaka-u.ac.jp

Received: 11 July 2003
Revised: 12 February 2004
Accepted: 13 April 2004

Abstract

Background Safety issues are of paramount importance in clinical human gene therapy. From this point of view, it would be better to develop a novel non-viral efficient gene transfer method. Recently, it was reported that ultrasound exposure could induce cell membrane permeabilization and enhance gene expression.

Methods In this study, we examined the potential of ultrasound for gene transfer into the kidney. First, we transfected rat left kidney with luciferase plasmid mixed with microbubbles, Optison, to optimize the conditions (duration of ultrasound and concentration of Optison). Then, 4, 7, 14 and 21 days after gene transfer, luciferase activity was measured. Next, localization of gene expression was assessed by measuring luciferase activity and green fluorescent protein (GFP) expression. Expression of GFP plasmid was examined under a fluorescence microscope at 4 and 14 days after gene transfer. Finally, to examine the side effects of this gene transfer method, biochemical assays for aspartate aminotransferase (AST), alanine aminotransferase (ALT), blood urea nitrogen (BUN) and creatinine (Cre) were performed.

Results Optison and/or ultrasound significantly enhanced the efficiency of gene transfer and expression in the kidney. Especially, 70–80% of total glomeruli could be transfected. Also, a significant dose-dependent effect of Optison was observed as assessed by luciferase assay (Optison 25%: 12.5×10^5 relative light units (RLU)/g tissue; 50%: 31.3×10^5 RLU/g tissue; 100%: 57.9×10^5 RLU/g tissue). GFP expression could be observed in glomeruli, tubules and interstitial area. Results of blood tests did not change significantly after gene transfer.

Conclusions Overall, an ultrasound-mediated gene transfer method with Optison enhanced the efficiency of gene transfer and expression in the rat kidney. This novel non-viral method may be useful for gene therapy for renal disease. Copyright © 2004 John Wiley & Sons, Ltd.

Keywords gene therapy; kidney; ultrasound; microbubble

Introduction

Gene therapy through the delivery of genetic constructs is emerging as a revolutionary and promising form of therapy for the treatment of human diseases. For diseases involving the kidney, gene therapy to replace dysfunctional genes or to suppress the production of disease mediators represents a promising new therapeutic approach. Gene therapy was originally proposed

in the late 1980s as a treatment strategy for diseases caused by single gene defects, such as cystic fibrosis or adenosine deaminase deficiency (ADA) [1]. Because the molecular tools for genetic manipulation were available, effectiveness seemed guaranteed. However, there were problems with gene delivery, with failure to achieve therapeutic levels of transgene expression. With these setbacks came the realization that diseases are complex multigene phenomena, hat more basic research is required before moving to clinical trials, and that clinical trials of gene therapy must be more rigorously controlled.

Renal disease has been considered one of the target diseases for gene therapy since, even now, there is no satisfactory pharmacological treatment to prevent and cure the process leading to end-stage renal failure [2,3]. The rapid development of gene transfer technology provides an opportunity to study the biological effects of different genes in the kidney and to develop treatment for various inherited or acquired renal diseases [4–9]. Several strategies have been developed to deliver foreign genes into different segments of the nephron using viral or non-viral vectors as well as genetically modified renal cells [10–17]. The use of conventional liposomes and viral vectors for transfecting genes into the human kidney is limited in terms of safety and efficiency. Therefore, several modified approaches have been developed.

We have developed the hemagglutinating virus of Japan (HVJ)-liposome-mediated gene transfer method for *in vivo* gene transfer into the kidney [10–13]. Although this method is easy to manipulate and highly efficient, and there is no limitation to the size of the vector DNA and little toxicity [18,19], its clinical utility such as large-scale production is still limited. Several studies have shown that ultrasound, used either alone or in combination with ultrasound contrast agents, can increase cell membrane permeability to macromolecules such as plasmid DNA [20–24]. This phenomenon has been referred to as sonoporation [20]. Most sonoporation studies have been carried out on cultured cells [20–25] or tumors *in vivo* [26–29], or skeletal muscle [30–32]. Moreover, recently we have found that this approach is applicable to gene transfer into the artery [33]. However, to our knowledge, there has been no previous investigation of whether ultrasound is able to enhance plasmid-mediated gene transfer into the kidney. Although based on this background we have already published two papers [34,35], in those studies we did not optimize the condition for gene transfer. Thus, in this study, we tried to develop and optimize a successful *in vivo* gene transfer method into the kidney using ultrasound exposure with microbubble material (Optison). Therefore, the global objective of our study was to investigate the potential usefulness of ultrasound as a method for improving the efficiency of plasmid-mediated gene transfer into the kidney, utilizing luciferase and green fluorescent protein (GFP) plasmid.

Materials and methods

Plasmid DNA

Luciferase expression plasmid was obtained from Promega Corporation (Madison, WI, USA). In this plasmid, firefly luciferase cDNA is driven by the SV 40 promoter and enhancer. GFP plasmid was obtained from BD Biosciences Clontech (Palo Alto, CA, USA). This plasmid contains the CMV promoter. As a control, we used a control plasmid that contained neither luciferase nor GFP cDNA.

Gene transfer into kidney by ultrasound

Eight-week-old male Wistar rats weighing 150 g were purchased from Charles River Japan (Osaka, Japan). Plasmid was transfected into the kidney via the renal artery using an ultrasound-mediated system. The procedure for the ultrasound-based gene transfer technique includes: (1) mixing luciferase or GFP or the control plasmids with Optison (Mallinckrodt, St. Louis, MO, USA) in several v/v ratios and injecting the mixed solution containing 50 μg of plasmid in 0.5 ml into the left renal artery with temporary clipping of the renal artery and vein (<5 min); (2) applying the ultrasound transducer (Rich-Mar, Inola, OH, USA) directly onto one side of the left kidney with a continuous-wave output of 1 MHz ultrasound at 5% power output, for a total of 60 s at 30-s intervals; (3) turning over the kidney and treating the other side with ultrasound using the same procedure. The infusion cannula is then removed, blood flow to the renal artery restored by release of the ligatures, and the wound closed.

Luciferase activity assay

Rats were killed at 4, 7, 14 and 21 days after gene transfer. Kidney samples were rapidly frozen in liquid nitrogen and homogenized in lysis buffer. The tissue lysates were briefly centrifuged (3000 rpm, 10 min), and 20 μl of supernatant were mixed with 100 μl of luciferase assay reagents. Firefly luciferase activity was measured for 1 min using a luciferase assay system (PicaGene; Tokyo-Inki, Tokyo, Japan). The values for luciferase activity shown in this paper were adjusted by the tissue weight. So values are expressed as relative light units (RLU)/g tissue.

Examination of GFP expression

To detect expression of GFP in injected kidney, kidneys were halved on day 4 after gene transfer, placed in liquid nitrogen and embedded in OTC compound. Then the kidneys were sectioned on a cryostat (6-μm sections).

Sections were examined for GFP using fluorescence microscopy with a fluorescein filter set.

Preparation of HVJ-liposomes

HVJ-liposomes were prepared in an identical fashion to that previously described [10–13,36,37]. Phosphatidylserine, phosphatidylcholine, and cholesterol were mixed in a weight ratio of 1 : 4.8 : 2 [10–13,36,37]. The lipid mixture (10 mg) was deposited on the sides of a flask by removal of tetrahydrofuran in a rotary evaporator. Dried lipid was hydrated in 200 μl balanced salt solution (BSS; 137 mM NaCl, 5.4 mM KCl, 10 mM Tris-HCl, pH 7.6) containing 50 μg of luciferase or GFP or the control plasmid. Liposomes were prepared by shaking and sonication. Purified HVJ (Z strain) was inactivated by UV irradiation (110 erg/nm^2/s) for 3 min just before use. The liposome suspension (0.5 ml, containing 10 mg lipids) was mixed with HVJ (30 000 hemagglutinating units) in a total volume of 4 ml BSS. The mixture was incubated at 4 °C for 5 min and then for 30 min with gentle shaking at 37 °C. Free HVJ was removed from the HVJ-liposomes by sucrose density gradient centrifugation. The top layer of the sucrose gradient was collected for use [10–13,36,37].

Collection of glomeruli

Glomeruli were isolated from the outer renal cortex of gene-transfected rats by means of a sieving technique (passing the cortical pulp through calibrated sieves of 180, 125 and 63 μm, respectively, as described previously [38]).

Histological analysis

Animals were killed under injection of sodium pentobarbital (50 mg/kg i.p.) on day 14 after gene transfer. The kidneys were fixed in 4% paraformaldehyde after perfusion with phosphate-buffered saline (PBS), and 5-μm-thick paraffin sections were stained with hematoxylin and eosin (HE). All HE-stained sections were evaluated by three investigators with no knowledge of experimental treatments. To assess the histological damage we followed the method described previously [39].

Measurement of plasma parameters

To examine the side effects of administration of microbubbles combined with ultrasound exposure, serum aspartate aminotransferase (AST), alanine aminotransferase (ALT), blood urea nitrogen (BUN) and creatinine (Cre) were measured after the rats had been killed. These levels were determined using a commercially available assay kit (Sigma Chemical Co., St. Louis, MO, USA) with a modification of the assay protocol suggested by the supplier.

RT-PCR analysis

Using reverse transcriptase polymerase chain reaction (RT-PCR) analysis on isolated glomeruli and the remaining parts of the kidney, we further examined whether expression of the transfected reporter plasmid could be observed in the glomerulus and the remaining parts of the kidney on day 21 after gene transfer. Total RNA (glomeruli and remaining parts) extracted from gene-transfected kidneys was subjected to RT-PCR analysis using two primers specific for luciferase DNA, GCC TGA AGT CTC TGA TTA AGT and ACA CCT GCG TCG AAG T, which yield 96-bp fragments [40]. The cycles were 94 °C for 30 s, 58 °C for 1 min, and 72 °C for 1 min. After 35 cycles, the PCR product was analyzed as well as samples amplified using GAPDH primers, which served as the internal control. GAPDH primers were purchased from Clontech Inc. (Palo Alto, CA, USA).

Statistical analysis

All values are expressed as mean ± SEM. Analysis of variance with a subsequent Bonferroni/Dunnet's test was employed to determine the significance of differences in multiple comparisons. Values of $p < 0.05$ were considered statistically significant.

Results

A series of preliminary studies were performed in normal rats in which the left kidney was perfused with luciferase plasmid or control plasmid, and Optison mixture accompanied by ultrasound exposure. First, we tried to determine the optimal duration of ultrasound exposure. Fifty micrograms of luciferase reporter plasmid were dissolved in 0.5 ml saline containing echocardiographic contrast agent, Optison, at two different concentrations (25 and 50%, v/v; n = 4 for each concentration) and infused into the left kidney through the renal artery. The kidney was then exposed to ultrasound for 1 or 2 min as detailed 'Materials and methods'. Luciferase activity assay was performed on day 4 after gene transfer. As shown in Figure 1a, there were no significant differences between exposure times at both concentrations of Optison (25 and 50%, v/v). From this result, we decided to use 1 min for exposure of ultrasound. Of course, no luciferase activity was observed in kidneys transfected with control plasmid (data not shown). The next step was to determine the optimal concentration of Optison. Several different concentrations of Optison (0, 5, 10, 25, 50 and 100%, v/v) with ultrasound exposure for 1 min were used, and luciferase activity was examined on day 4 after gene transfer. In this experiment, a dose-dependent effect of Optison was observed, as shown in Figure 1b. However, at higher concentrations of Optison, such as 50 or 100% (v/v), histological damage on day 14 after gene transfer could be seen in the

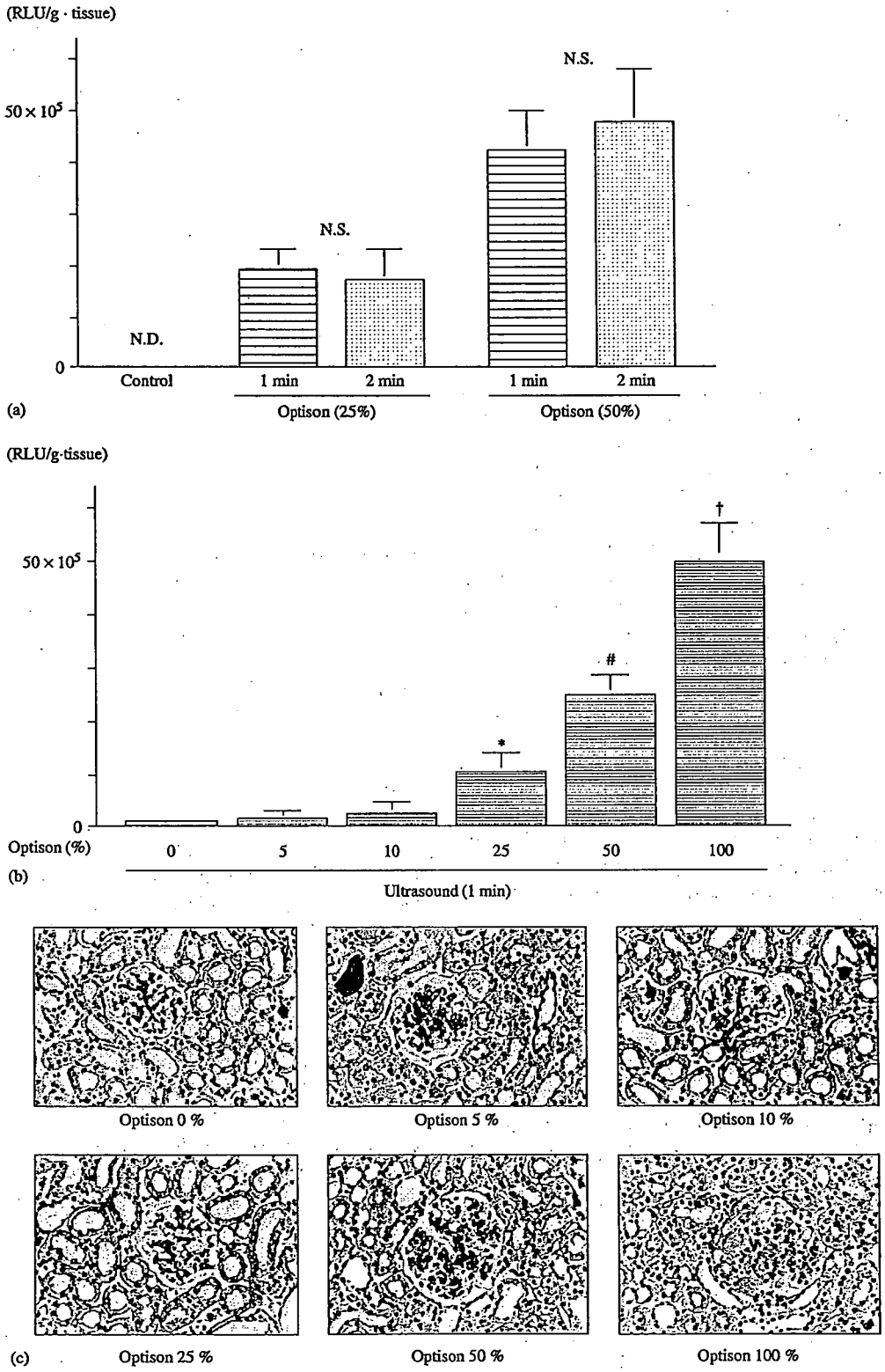

Figure 1. (a) Luciferase activity in kidney on day 4 after gene transfer to examine the effect of ultrasound exposure time. 1 min and 2 min indicate the ultrasound exposure time. Control = kidneys with no gene transfer. N.S. = not significant. RLU = relative light units. Concentrations of Optison are expressed as v/v. n = 5 per group. Data are calculated from five independent experiments. The total amount of transfected plasmid per one kidney was 50 μg. (b) Luciferase activity in kidney on day 4 after gene transfer to examine the effect of Optison concentration. In this experiment, ultrasound exposure was 1 min. Concentrations of Optison are expressed as v/v. $^*p < 0.01$ vs. Optison 0%, and $\#p < 0.01$ vs. Optison 25% and 50%. RLU = relative light units. n = 5 per group. Data are calculated from five independent experiments. The total amount of transfected plasmid per one kidney was 50 μg. (c) Representative photograph of kidneys on day 14 after gene transfer. In this experiment, ultrasound exposure was 1 min. Concentrations of Optison are expressed as v/v. n = 5 per group. The total amount of transfected plasmid per one kidney was 50 μg

Table 1. Blood test data (AST, ALT, BUN and Cre) on day 4 after gene transfer. In this experiment, ultrasound exposure was 1 min. 0%, 5%, 10%, 25%, 50% and 100% are the concentrations of Optison expressed as v/v. Values indicate mean ± SE. There were no significant differences between each group. n = 6 per group. Data are calculated from five independent experiments. The total amount of transfected plasmid per one kidney was 50 μg

Optison	0%	5%	10%	25%	50%	100%
AST (IU/l)	142 ± 19	207 ± 28	184 ± 19	192 ± 21	203 ± 24	186 ± 21
ALT (IU/l)	59 ± 8	68 ± 9	57 ± 7	62 ± 9	69 ± 7	57 ± 8
BUN (mg/dl)	12.1 ± 1.3	14.2 ± 1.9	11.7 ± 2.0	14.8 ± 1.5	13.9 ± 1.7	13.2 ± 1.5
Cre (mg/dl)	0.2 ± 0.03	0.3 ± 0.05	0.4 ± 0.02	0.3 ± 0.05	0.3 ± 0.02	0.4 ± 0.03

kidneys, even though plasma parameters of hepatic and renal function did not change, as shown in Figure 1c and Table 1. Representative photographs of kidneys transfected with luciferase plasmid mixed with Optison at the concentrations of 50 and 100% (v/v) clearly showed glomerular damage, as shown in Figure 1c. Also, quantitative analysis for histological damage in glomeruli supported this fact. Significant damage, such as matrix expansion and increase in glomerular diameter, was observed in kidneys infused with 50 and 100% (v/v) Optison (data not shown). Moreover, although we do not show here the data from control kidneys transfected with control plasmid, the same extent of damage could be seen in the sections. From these results we can easily speculate that renal damage seen in rats might be due to the high concentration of Optison. These data led us to decide to use a concentration of Optison of 25% (v/v) which showed an apparently significant effect on gene expression of the luciferase reporter gene.

Then, we examined how long the expression would last. Rats whose kidneys were transfected with luciferase plasmid with 25% Optison (v/v) accompanied by ultrasound exposure for 1 min were sacrificed on days 7, 14 and 21 days after gene transfer. As shown in Figure 2, the peak gene expression was seen on day 7; however, significant gene expression in the kidney lasted until at least day 21 after gene transfer. Moreover, there were no significant changes in plasma parameters during the observation period. The data of plasma parameters (AST, ALT, BUN, Cre) at 0 (Pre), 7, 14 and 21 days after gene transfer are shown in Table 2. As shown here, the gene transfer method mediated by ultrasound and Optison (less than 25%, v/v) was safe and efficient. We did not detect luciferase activity from kidneys transfected with control plasmid at each time point (data not shown).

The next question was the site where gene expression occurred. We isolated the glomeruli and performed a luciferase assay using isolated glomeruli and the remaining parts of the kidney. Interestingly, both glomeruli and the remaining parts of the kidney showed reporter gene expression at least until day 21 after gene transfer, as shown in Figure 3a. To enhance this result, we performed RT-PCR for luciferase in the same samples. As shown in Figure 3b, RNA expression could be detected on day 21 after gene transfer. From these data, we confirmed that gene expression induced by gene transfer mediated by Optison and ultrasound exposure was detected in both glomeruli and the remaining parts

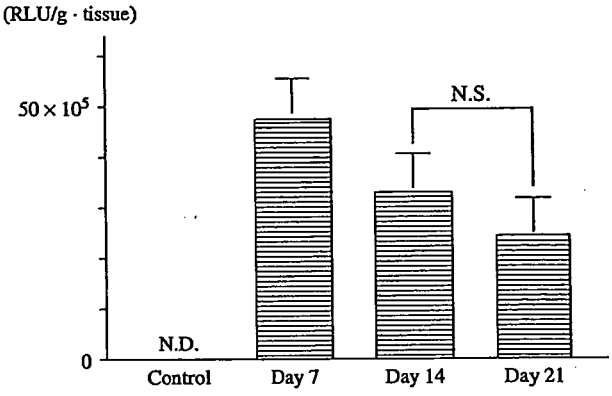

Figure 2. Luciferase activity in kidney after gene transfer. Assays were performed on days 7, 14 and 21 after gene transfer. In this experiment, ultrasound exposure was 1 min and the concentration of Optison was 25% (v/v). Control means kidney before gene transfer. N.D. = not detected. N.S. = not significant. n = 6 per group. Data are calculated from five independent experiments. The total amount of transfected plasmid per one kidney was 50 μg

Table 2. Blood test data (AST, ALT, BUN and Cre) after gene transfer. In this experiment, ultrasound exposure was 1 min and the concentration of Optison was 25% (v/v). Assays were performed on days 7, 14 and 21 after gene transfer and before gene transfer. Values indicate mean ± SE. There were no significant differences between each group. n = 6 per group. Data are calculated from five independent experiments. The total amount of transfected plasmid per one kidney was 50 μg

	Pre	Day 7	Day 14	Day 21
AST (IU/l)	142 ± 19	207 ± 28	184 ± 19	192 ± 21
ALT (IU/l)	59 ± 8	68 ± 9	57 ± 7	62 ± 9
BUN (mg/dl)	12.1 ± 1.3	14.2 ± 1.9	11.7 ± 2.0	14.8 ± 1.5
Cre (mg/dl)	0.2 ± 0.03	0.3 ± 0.05	0.4 ± 0.02	0.3 ± 0.05

of the kidney as assessed by RT-PCR and protein assay. In this RT-PCR assay we showed the positive control as indicated as P in Figure 3b. RNA was extracted from the fibroblasts and luciferase plasmid was over-expressed (Promega Corporation).

Moreover, to visualize the expression of the transfected gene, we examined GFP plasmid expression transfected by this new technique with the same approach as shown above. On days 4 and 14 after gene transfer, frozen sections of the kidneys were observed by fluorescence microscopy. As shown in Figure 4, in both glomeruli and the remaining parts of the kidney such as tubules or interstitial tissue, fluorescence was detected, suggesting

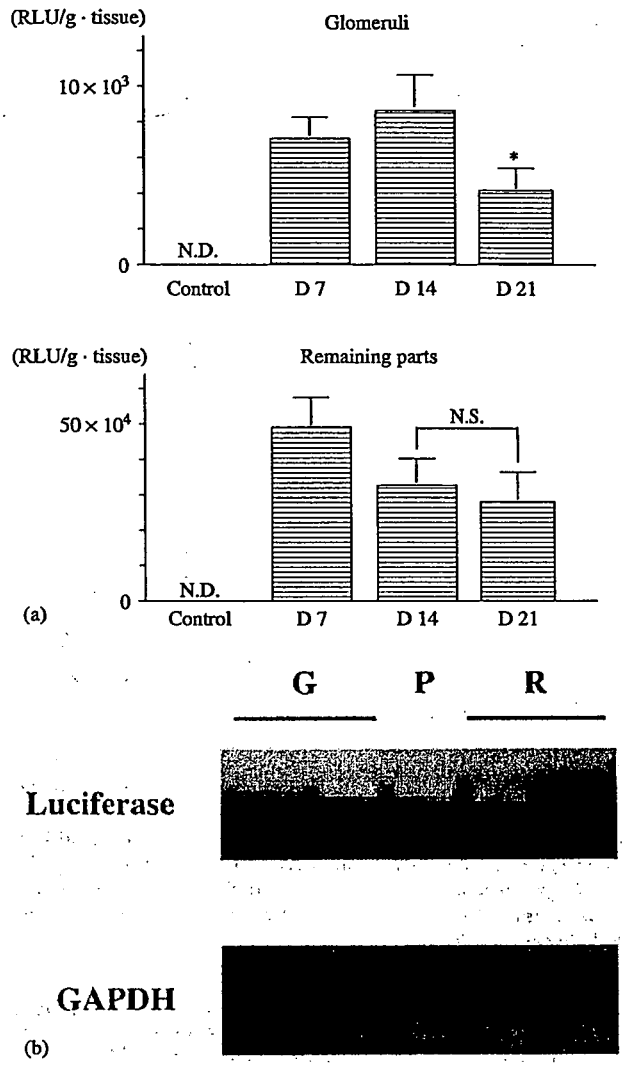

Figure 3. (a) Luciferase activity in kidney (glomeruli and remaining parts of kidney (interstitial tissue and tubules)) on days 7, 14 and 21 after gene transfer. In this experiment, ultrasound exposure was 1 min and the concentration of Optison was 25% (v/v). Isolation of glomeruli was performed as described in 'Materials and methods'. Control = control kidney which had no gene transfer. D7, D14 and D21 = days 7, 14 and 21 after gene transfer, respectively. *$p < 0.01$ vs. D14. N.S. = not significant. n = 6 per group. Data are calculated from five independent experiments. The total amount of transfected plasmid per one kidney was 50 μg. (b) Representative photograph of RT-PCR performed on RNA samples extracted on day 21 after gene transfer. In this experiment, ultrasound exposure was 1 min and the concentration of Optison was 25% (v/v). G = glomeruli, P = positive control and R = remaining parts of the kidney. In lanes G and R there two different bands from different samples, respectively. The total amount of transfected plasmid per one kidney was 50 μg

that the transfected GFP plasmid was expressed in these areas. In control kidneys transfected with control plasmid on days 4 and 14 no fluorescence could be observed (Figures 4B and 4D). There seemed to be no significant changes between the distribution pattern of fluorescence in kidneys on days 4 and 14. This fact is almost consistent with results of luciferase activity.

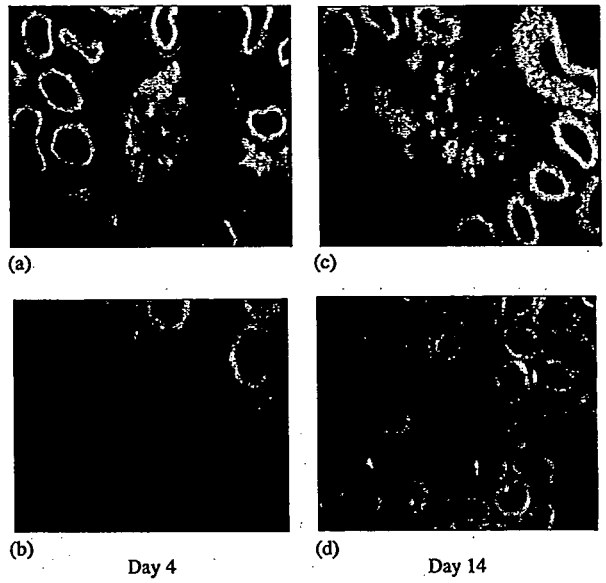

Figure 4. Representative photographs of kidney transfected with GFP plasmid on day 14 after gene transfer. In this experiment, ultrasound exposure was 1 min and the concentration of Optison was 25% (v/v). Kidney samples were collected on days 4 and 14 after gene transfer. Photographs of (A) left kidney transfected with GFP plasmid on day 4; (B) right kidney of control which had no gene transfer on day 4; (C) left kidney transfected with GFP plasmid on day 14; and (D) right kidney of control which had no gene transfer on day 14. The total amount of transfected plasmid per one kidney was 50 μg

Finally, we compared the efficiency of gene transfer by this new method with that of the HVJ-liposome method, which we previously reported as an efficient gene transfer method to the kidney [10–13]. The HVJ-liposome method is based on liposomes with inactivated virus. From this point of view, the HVJ-liposome method has many hurdles before application in clinical trials. We must develop an efficient and safe gene transfer method aimed at application in human trials. As shown in Figure 5, ultrasound (1 min) itself enhanced gene expression. However, compared with the HVJ-liposome method, the level of gene expression just with ultrasound was still significantly less (ultrasound: 1.37 ± 0.14 0215 10^4 RLU/g tissue; HVJ-liposome: $2.69 \pm 0.28 \times 10^4$ RLU/g tissue). On the other hand, the combination of Optison (25%, v/v) and ultrasound exposure (1 min) significantly enhanced gene expression compared with the HVJ-liposome method (Optison + ultrasound: $17.45 \pm 1.82 \times 10^4$ RLU/g tissue; HVJ-liposome: $2.69 \pm 0.28 \times 10^4$ RLU/g tissue, $p < 0.01$).

Discussion

Gene therapy is now moving from experimental studies to clinical applications. It could be applicable not only as therapy for inherited diseases, but also as new treatments for acquired diseases. However, one of the limiting steps in gene therapy is the gene transfer

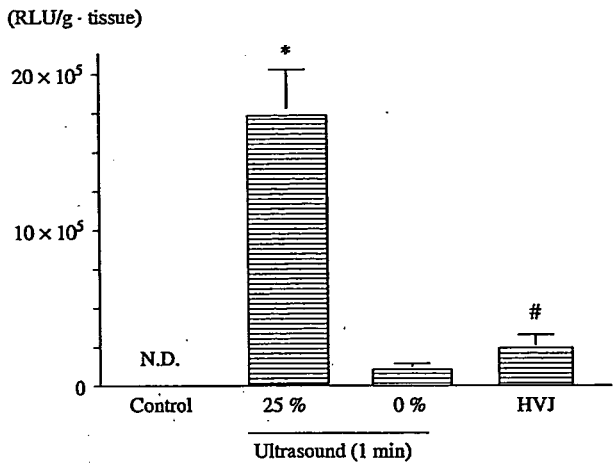

Figure 5. Comparison of gene expression with the HVJ-liposome method. To perform this experiment, luciferase plasmid was used. Luciferase activity assay was performed on day 4 after gene transfer using the whole kidney. The concentration of Optison was 25% (v/v). Control = kidney with no gene transfer. 1 min and 0 min indicate the ultrasound exposure time, respectively. HVJ = kidney transfected with luciferase plasmid by HVJ-liposome method. N.D. = not detected. *$p < 0.01$ vs. 0 min and HVJ, respectively. #$p < 0.01$ vs. 0 min. n = 6 per group. Data are calculated from five independent experiments. The total amount of transfected plasmid per one kidney was 50 μg

method. Several strategies have been developed to deliver foreign genes into different segments of the nephron, using viral and non-viral vectors as well as genetically modified renal cells [10,17,41–45]. Generally, gene expression by non-viral vectors is transient and rather weak, while genetically modified renal cells trapped in the kidney could potentially induce additional biological effects. On the other hand, genetically modified cell vectors are not practical. Although viral vectors such as adenoviral vectors, retroviral vectors or adeno-associated viral vectors yield higher gene expression, these vectors have unfavorable effects on the host body such as immunosuppression or oncogenesis [46,47]. In the present study, we established an easy, safe and efficient gene transfer method mediated by ultrasound and microbubbles. GFP expression, which indicates successful transfection of foreign genes, could be observed in more than 70–80% of total glomeruli and most tubular cells in the kidney treated with the ultrasound and Optison-mediated transfer method. In contrast, the ratio of glomeruli transfected with the reporter gene to total glomeruli was at most 30% with the HVJ-liposome method [10,42]. Although in the present study we did not compare the efficiency of this method with that of another method, judging from the previously published data, transfection efficiencies of other methods may not be as high as that of this novel transfer method, even though this was evaluated from the values published already. This method should be quite impressive for future clinical applications and have potential as a new treatment strategy.

In contrast to the efficiency of this new method, overexposure to ultrasound, which may cause irreversible tissue injury, should be considered as a critical issue, and it is important to establish the optimal conditions for this method. In the present study, we demonstrated that ultrasound exposure did not change gene expression up to 2 min. Because longer ultrasound exposure may cause organ damage, we did not examine exposure times longer than 2 min. Moreover, injection of plasmid DNA into muscle is known to induce mild inflammatory damage, which has been linked to the presence of proinflammatory unmethylated CpG motifs within prokaryotic DNA [48,49]. However, we did not observe even a mild degree of inflammation in the kidney after gene transfer. Of note, ultrasound itself was not associated with any increase in damage or inflammation in the kidney as long as the exposure time was less than 1 min (data not shown).

In addition to ultrasound exposure, the use of Optison at higher concentrations (50 or 100%, v/v) led to severe injury as assessed histologically. Accordingly, we applied ultrasound exposure for 1 min, and Optison at a concentration of 25%. Thus, we decided the optimal conditions for this newly developed gene transfer method into the kidney, which should be of great value for the clinical application of this method. It has been previously reported that ultrasound exposure increased the efficiency of gene transfer into cultured cells, and its mechanism of action is thought to be increased cell membrane porosity [20–25]. Consistent with previous studies, the present study demonstrated that ultrasound exposure increased reporter gene expression in the kidney, however, the level was not as high as reported. We therefore modified the procedure using microbubbles, Optison, to increase the reporter gene expression, as previously reported [30,33]. This concept is based on the previous observation that microbubbles, that contain gas bodies filled with perfluoropropane, lowered the threshold for the production of acoustic cavitation and enhanced the sonoporation of cultured cells with ultrasound exposure. Of interest, other echo contrast agents such as Levovist, which contains air-based gas bodies with a different stabilization strategy, and Hexabrix, which does not contain gas bodies, did not enhance gene expression (data not shown). Optison contains about 5×10^8/ml gas bodies, 2–4.5 μm in diameter, which are filled with perfluoropropane and stabilized by a solid shell of heat-denatured human albumin [50,51]. Although further studies are needed to investigate the exact molecular mechanism by which Optison enhances transfection efficiency, the molecular structure of gas-filled microspheres and their contents may be implicated in the mechanisms of action.

Not all viral vectors, for example, adeno-associated viral vectors, are able to accommodate the full-length target gene to be transfected. An alternative approach is to use a non-viral vector such as plasmid DNA, which is less toxic, cheaper, easier to prepare, and able to accommodate the full-length target cDNA. However, the major drawback of the naked DNA approach up to now has been the

very low gene transfer efficiency compared with viral vectors. The use of ultrasound as an adjuvant measure to enhance plasmid DNA delivery has a number of advantageous features, which should increase the overall prospects for therapeutic application of naked DNA in the kidney. It is true that electroporation-mediated gene transfer resulted in rather high gene expression [52–54]. However, in contrast to electroporation, ultrasound is a non-painful and well-established tool in clinical medicine. The non-invasive nature of ultrasound and the absence of neutralizing antibodies against plasmid DNA also raise the possibility that treatment could be easily repeated on a relatively frequent basis. Lastly, ultrasound-mediated destruction of intravascularly injected microbubbles has been used to induce microvessel breaches that are large enough to permit extravasation of macromolecules, including plasmid DNA [55]. Therefore, ultrasound could be a powerful adjunct to intravascular delivery of plasmid DNA into the kidney. Further studies will be required to investigate the full therapeutic potential of ultrasound-mediated approaches to gene delivery in the setting of kidney disease.

Acknowledgements

We wish to thank Keiko Izawa for her excellent technical assistance and Dr. Phil Taso at Stanford University for his excellent technical advice. This work was partially supported by grants from the Japan Health Sciences Foundation, a Grant-in-Aid from The Ministry of Public Health and Welfare, a Grant-in-Aid for the Development of Innovative Technology, a Grant-in-Aid from Japan Promotion of Science, Special Coordination Funds of the Ministry of Education, Culture, Sports, Science and Technology, the Japanese Government, a grant from the Osaka Kidney Foundation (OKF02-0008), and a grant from KANAE Foundation for Life & Socio-Medical Science.

References

1. Blease RM, Culver KW, Miller AD, *et al.* T lymphocyte directed gene therapy for ADA-SCID: Initial trial results after 4 years. *Science* 1995; **270**: 475–480.
2. Bakris GL. Hypertension and nephropathy. *Am J Med* 2003; 115: 49S–54S.
3. Nissenson AR. Disease management improves outcomes in patients with CKD. *Nephrol News Issues* 2003; 17: 15–19.
4. Kitamura M. Transfer of exogenous genes into the kidney. *Exp Nephrol* 1994; 2: 313–317.
5. Riley DJ, Lee WH. The potential gene therapy for treatment of kidney diseases. *Semin Nephrol* 1995; 15: 57–69.
6. Fine LG. Gene transfer into the kidney: Promise for unraveling disease mechanisms, limitations for human gene therapy. *Kidney Int* 1996; 49: 612–619.
7. Lipkowitz MS, Klotman ME, Bruggeman LA, *et al.* Molecular therapy for renal diseases. *Am J Kidney Dis* 1996; 28: 475–492.
8. Imai E, Isaka Y. Strategies of gene transfer to the kidney. *Kidney Int* 1998; 53: 264–272.
9. Kone BC. How will gene therapy apply to the kidney in the 21st century? *Semin Nephrol* 2000; 20: 47–59.
10. Tomita N, Higaki J, Morishita R, *et al.* Direct *in vivo* gene introduction into rat kidney. *Biochem Biophys Res Commun* 1992; 186: 129–134.
11. Tomita N, Morishita R, Tomita S, *et al.* Transcription factor decoy for NFκB inhibits TNF-α-induced cytokine and adhesion molecules expression *in vivo*. *Gene Ther* 2000; 7: 1326–1332.
12. Tomita N, Morishita R, Lan HY, *et al.* *In vivo* administration of a nuclear factor-kappa B decoy suppressed experimental crescentic glomerulonephritis. *J Am Soc Nephrol* 2000; 11: 1244–1252.
13. Tomita N, Morishita R, Yamamoto K, *et al.* Target gene therapy for rat glomerulonephritis using HVJ-immunoliposomes. *J Gene Med* 2002; 4: 527–535.
14. Heikkila P, Parpala T, Lukkarinen O, *et al.* Adenovirus-mediated gene transfer into kidney glomeruli using an *ex vivo* and *in vivo* kidney perfusion system – first steps towards gene therapy of Alport syndrome. *Gene Ther* 1996; 3: 21–27.
15. Zhu G, Nicolson AG, Cowley BD, *et al.* *In vivo* adenovirus-mediated gene transfer into normal and cystic rat kidneys. *Gene Ther* 1996; 3: 298–304.
16. Lipkowitz MS, Hanss B, Tulchin N, *et al.* Transduction of renal cells *in vitro* and *in vivo* by adeno-associated virus gene therapy vectors. *J Am Soc Nephrol* 1999; 10: 1908–1915.
17. Kitamura M, Taylor S, Unwin R, *et al.* Gene transfer into rat renal glomerulus via a mesangial cell vector: site-specific delivery *in situ* amplification and sustained expression of an exogenous gene *in vivo*. *J Clin Invest* 1994; 94: 497–505.
18. Kaneda Y, Morishita R, Tomita N. Increased expression of DNA cointroduced with nuclear protein in adult rat liver. *J Mol Med* 1995; 73: 289–297.
19. Kaneda Y, Saeki Y, Morishita R. Gene therapy using HVJ-liposomes: the best of both worlds? *Mol Med Today* 1999; 5: 298–303.
20. Kim HJ, Greenleaf JF, Kinnick RR, *et al.* Ultrasound-mediated transfection of mammalian cells. *Hum Gene Ther* 1996; 7: 1339–1346.
21. Bao S, Thrall BD, Miller DL. Transfection of a reporter plasmid into cultured cells by sonoporation *in vitro*. *Ultrasound Med Biol* 1997; 23: 953–959.
22. Lauer U, Burgelt E, Sqiure Z, *et al.* Shockwave permeabilization as a new gene transfer method. *Gene Ther* 1997; 4: 710–715.
23. Tata DB, Dunn F, Tindall DJ. Selective clinical ultrasound signals mediate differential gene transfer and expression in two human prostate cancer cells lines; LnCap and PC-3. *Biochem Biophys Res Commun* 1997; 234: 64–67.
24. Wyber JA, Andrews J, D'Emanuele A. The use of sonication for the efficient delivery of plasmid DNA into cells. *Pharm Res* 1997; 14: 750–756.
25. Tachibana K, Uchida T, Ogawa K, *et al.* Induction of cell-membrane porosity by ultrasound. *Lancet* 1999; 353: 1409.
26. Bao S, Thrall B, Gies RA, *et al.* *In vivo* transfection of melanoma cells by lithotripter shock waves. *Cancer Res* 1998; 58: 219–221.
27. Anwer K, Kao G, Proctor B, *et al.* Ultrasound enhancement of cationic lipid-mediated gene transfer to primary tumors following systemic administration. *Gene Ther* 2000; 7: 1833–1839.
28. Huber PE, Pfisterer P. *In vitro* and *in vivo* transfection of plasmid DNA in the Dunning prostate tumor R3327-AT1 is enhanced by focused ultrasound. *Gene Ther* 2000; 7: 1516–1525.
29. Manome Y, Nakamura M, Ohno T, *et al.* Ultrasound facilitates transfection of naked plasmid DNA into colon carcinoma cells *in vitro* and *in vivo*. *Hum Gene Ther* 2000; 11: 1521–1528.
30. Taniyama Y, Tachibana K, Hiraoka K, *et al.* Development of safe and efficient novel nonviral gene transfer using ultrasound: enhancement of transfection efficiency of naked plasmid DNA in skeletal muscle. *Gene Ther* 2002; 9: 372–380.
31. Lu QL, Liang HD, Partridge T, *et al.* Microbubble ultrasound improves the efficiency of gene transduction in skeletal muscle *in vivo* with reduced tissue damage. *Gene Ther* 2003; 10: 396–405.
32. Schratzberger P, Krainin JG, Schratzberger G, *et al.* Transcutaneous ultrasound augments naked DNA transfection of skeletal muscle. *Mol Ther* 2002; 6: 576–583.
33. Taniyama Y, Tachibana K, Hiraoka K, *et al.* Local delivery of plasmid DNA into rat carotid artery using ultrasound. *Circulation* 2002; 105: 1233–1239.
34. Azuma H, Tomita N, Kaneda Y, *et al.* Transfection of NFκB decoy oligodeoxynucleotides using high efficient ultrasound-mediated gene transfer into the donor kidney prolonged survival of rat renal allograft. *GeneTher* 2003; 10: 415–425.
35. Lan HY, Mu W, Tomita N, *et al.* Inhibition of renal fibrosis by gene transfer of inducible Smad7 using ultrasound-microbubble system in rat UUO model. *J Am Soc Nephrol* 2003; 14: 1535–1548.

36. Tomita N, Higaki J, Kaneda Y, *et al.* Hypertensive rats produced by *in vivo* introduction of the human renin gene. *Circ Res* 1993; 73: 898–905.
37. Tomita N, Morishita R, Higaki J, *et al.* Transient decrease in high blood pressure by *in vivo* transfer of antisense oligonucleotide against rat angiotensinogen. *Hypertension* 1995; 26: 131–136.
38. Gonzalez R, Redon P, Lakhdar R, *et al.* Cyclosporine nephrotoxicity assessed in isolated human glomeruli and cultured mesangial cells. *Toxicol In Vitro* 1990; 4: 391–395.
39. Raji L, Azar S, Keane W. Mesangial immune injury, hypertension and progressive glomerular damage in Dhal rats. *Kidney Int* 1984; 26: 137–143.
40. Cok SJ, Morrison AR. The 3′-untranslated region of murine cyclooxygenase-2 contains multiple regulatory elements that alter message stability and translational efficiency. *J Biol Chem* 2001; 276: 23 179–23 185.
41. Bosch R, Woolf A, Fine L. Gene transfer into mammalian kidney: direct retrovirus-transduction of regenerating tubular epithelial cells. *Exp Nephrol* 1993; 1: 49–54.
42. Isaka Y, Fujiwara Y, Ueda N, *et al.* Glomerulosclerosis induced by *in vivo* transfection of transforming growth factor-β or platelet derived growth factor gene into the rat kidney. *J Clin Invest* 1993; 92: 2597–2601.
43. Moullier P, Friedlander G, Calise D, *et al.* Adenoviral-mediated gene transfer to renal tubular cells *in vivo*. *Kidney Int* 1994; 45: 1220–1225.
44. Kitamura M. Creation of a reversible on/off system for site-specific *in vivo* control of exogenous gene activity in renal glomerulus. *Proc Natl Acad Sci U S A* 1996; 93: 7387–7391.
45. Lai LW, Moeckel GW, Lien YH. Kidney-targeted liposome-mediated gene transfer in mice. *Gene Ther* 1997; 4: 426–431.
46. Gore ME. Adverse effects of gene therapy: gene therapy can cause leukaemia: no shock, mild horror but a probe. *Gene Ther* 2003; 10: 4.
47. Marshall E. Gene therapy death prompts review of adenovirus vector. *Science* 1999; 286: 2244–2245.
48. Jakob T, Walker PS, Krieg AM, *et al.* Activation of cutaneous dendritic cells by CpG-containing oligodeoxynucleotides: a role for dendritic cells in the augmentation of Th1 responses by immunostimulatory DNA. *J Immunol* 1998; 161: 3042–3049.
49. Hemmi H, Takeuchi O, Kawai T, *et al.* A Toll-like receptor recognizes bacterial DNA. *Nature* 2000; 408: 740–745.
50. Ward M, Wu J, Chiu JF. Ultrasound-induced cell lysis and sonoporation enhanced by contrast agents. *J Acoust Soc Am* 1999; 105: 2951–2957.
51. Miller DL, Quddus J. Diagnostic ultrasound activation of contrast agents gas bodies induces capillary rupture in mice. *Proc Natl Acad Sci U S A* 2000; 97: 10 179–10 184.
52. Tsujie M, Isaka Y, Nakamura H, *et al.* Electroporation-mediated gene transfer that targets glomeruli. *J Am Soc Nephrol* 2001; 12: 949–954.
53. Nakamura H, Isaka Y, Tsujie M, *et al.* Electroporation-mediated PDGF receptor-IgG chimera gene transfer ameliorates experimental glomerulonephritis. *Kidney Int* 2001; 59: 2134–2145.
54. Imai E, Isaka Y. Gene electrotransfer: potential for gene therapy of renal diseases. *Kidney Int* 2002; 61: S37–S41.
55. Price RJ, Skyba DM, Kaul S, *et al.* Delivery of colloidal particles and red blood cells to tissue through microvessels rupture created by targeted microbubble destruction with ultrasound. *Circulation* 1998; 98: 1264–1267.

Molecular Delivery into a Lipid Bilayer with a Single Shock Waves Using Molecular Dynamic Simulation

[1]Kenichiro Koshiyama, [2]Tetsuya Kodama, [3]Michael R. Hamblin, [3]Apostolos G. Doukas, [1]Takeru Yano, and [1]Shigeo Fujikawa

[1]*Division of Mechanical Science, Graduate School of Engineering, Hokkaido University Sapporo 060-8628,Japan.*
[2]*Biomedical Engineering Research Organization, Tohoku University, 2-1 Seiryo-machi, Aoba-ku Sendai 980-9575, Japan.*
[3]*Wellman Center for Photomedicine, Department of Dermatology, Massachusetts General Hospital, Harvard Medical School, 50 Blossom Street, Boston, MA02114, USA.*

Abstract. Cell permeabilization by shock waves may have application in gene therapy and anticancer drug delivery. In the present study we performed direct molecular dynamic (MD) simulation of the interaction of a single shock wave with a cell membrane to investigate the mechanism of the cell permeabilization. The shock wave was characterized by an impulse that was expressed with a velocity determined by the change in the momentum. The cell membrane was designed as a dipalmitoylphosphatidylcholine (DPPC) lipid bilayer placed between two layers of water molecules. The MD simulation determined the relationship between water penetration into the bilayer, the order parameter, the fluidity of each lipid molecule, and the intensity of impulse. These structural changes in the bilayer may be an important factor in the use of shock waves to produce transient membrane permeability.

INTRODUCTION

Cell permeabilization using shock waves may be a promising way of introducing macromolecules and small polar molecules into the cytoplasm, and may have applications in gene therapy and anticancer drug delivery. The pressure profile of a shock wave indicates its energy content, and shock propagation in tissue is associated with cellular displacement, leading to the development of cell deformation. Shock waves are nonlinear, finite-amplitude waves, and the flow induced behind the shock waves cannot be ignored. The duration of the particle motion is the order of the pulse duration, dt, of the shock wave, and the displacement, d, of the particle is about the order of $d = u_p \times dt$, where u_p is the induced speed, which is inversely proportional to the density of the particle. A rough estimate of tissue displacement obtained with a single shock wave generated by a clinical lithotripter is calculated to be 1-20 μm, using pressure data obtained in water [1]. This value is similar to that measured in rabbit liver resulting from a shock wave produced by detonation of an explosive micropellet (7-10 μm) [2]. Kodama et al.[3] reported that the shock wave impulse (defined as the integral of pressure with duration) is an important factor governing the temporary permeability increase in cell membranes necessary for delivering macromolecules into

CP754, *4th International Symposium on Therapeutic Ultrasound*
edited by G.R. ter Haar and I. Rivens

cells. The detailed mechanism of the transient membrane permeability increase is still unclear. In present study we conducted molecular dynamics (MD) simulations of the interaction of the shock wave impulse with a lipid bilayer to investigate the mechanism. In addition, we studied the structural change of the bilayer and subsequent characteristic delivery of water molecules into the bilayer.

METHOD

A cell membrane was designed as a 32 dipalmitoylphosphatidylcholine (DPPC) lipid bilayer, placed between two 1200 water layers in the calculation box. This box was a cuboid whose longitudinal axis was set to the z-axis perpendicular to the xy plane. The stable liquid-crystal phase bilayer was calculated for several tens of nano seconds with a constant temperature of 323K and pressure of 1 bar with periodic boundary conditions. The detailed calculation conditions are presented elsewhere [4]. The velocity and positions of molecules in the system were used as initial conditions for applying shock wave.

A single shock wave was applied downwards to a part of the upper water layer. The shock wave was characterized by an impulse that was expressed with a velocity V_2 determined by the change in the momentum in the upper water layer. The V_2 was calculated as

$$V_2 = \frac{I_P}{M} A \ , \tag{1}$$

where M (kg) is the mass of the water molecules in the upper layer, $A(m^2)$ is the area of the x-y plane in the calculation box, and I_P is the shock wave impulse from 1.6 to 16 mPa s (pressure times time) which corresponds to 0.1 to1.0 mPa s /lipid[5].

The simulations were performed using the AMBER 7 set of programmes [6].

RESULTS AND DISUCUSSION

Figure 1 shows the time evoloution of the structural change in the bilayer with an impulse of 0.7mPa· s. Water molecules in the stable state rarely penetrate into the hydrophobic region of the bilayer (Fig.1a). However, when the impulse was applied to the water region, a wave propagated into the bilayer, followed by movement of water molecules into the bilayer, and structural change occurred (Fig.1b-d). Table 1 shows the impulse intensity dependence of the number of water molecules delivered into the bilayer with the impulse, the averaged order parameter, and the lateral mass center velocity of all DPPC lipids. The number of delivered water molecules increased with increasing impulse intensity. This trend was in qualitatively good agreement with previously obtained experimental results. The averaged order parameter decreased with increasing impulse intensity and this meant the alkyl chain structure became disordered. Further, increase in the impulse intensity led to an increase in V_2, which means that each DPPC lipid moves faster than those in the stable state with increasing impulse intensity. Therefore, we concluded that the impulse might increase not only the penetrataion of water molecules into the bilayer, but also the disorder of the alkyol chain, and the fluidity of the lipid, which might be related to transient membrane permeability.

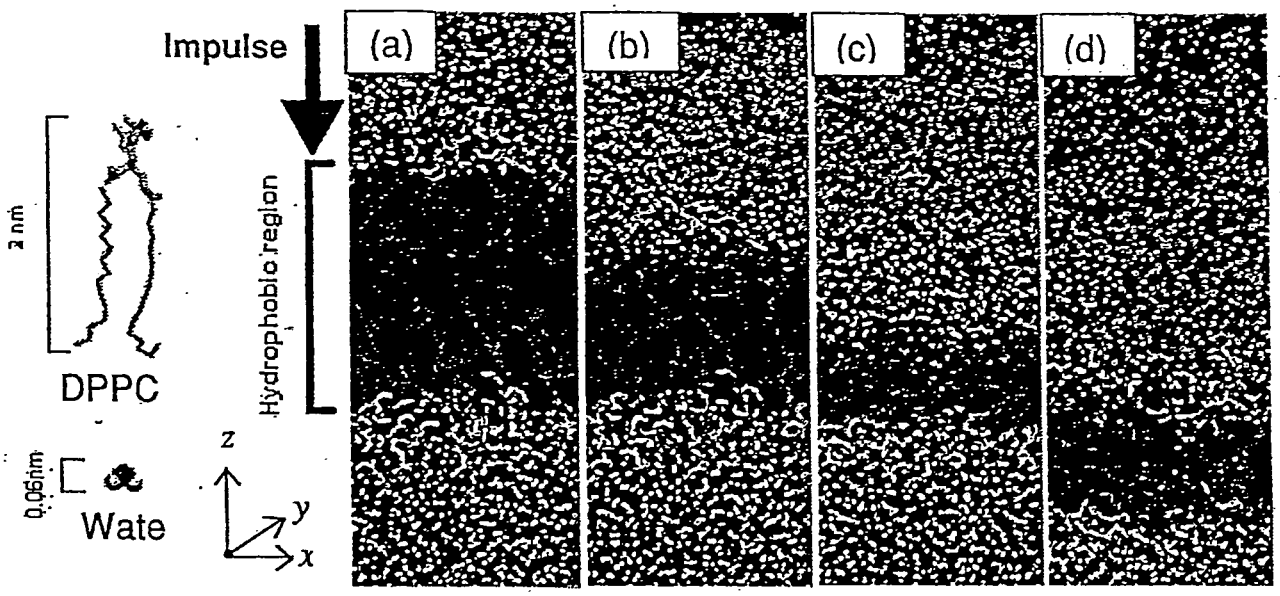

FIGURE 1. Structural change in the DPPC bilayer with an impulse of 0.7mPa s /lipid : The impulse is applied downwards to a part of the upper water layer. (a) Stable state, (b) 0.15ps, the upper water layer moves downwards, (c) 0.30 ps, the lower monolayer moves, (d) 0.45ps, the bilayer moves. All figures were made with the VMD molecular visualization programme[7]

TABLE 1. Uptake of water molecules into the lipid bilayer and its structure change due to a single shock wave impulse.

Impulse (mPa s)	N_W	S_{CD}	V_C
0	1	0.14	1
4.8	3	0.076	2
9.6	11	0.066	7
14.4	18	0.061	16

N_W : number of water molecules delivered into the bilayer normalized with the number of water molecule in the hydrophobic region of bilayer in the stable state, S_{CD} : averaged order parameter, V_C : lateral mass center velocity of DPPC lipids normalized with the velocity in the stable state.

CONCLUSION

We conducted MD simulations to elucidate the mechanism of the interaction of a shock wave impulse with a lipid bilayer. After exposure to the impulse, a structural change of the bilayer and subsequent increase in the fluidity of each molecule was induced. These changes in the bilayer may be an important factor in the use of shock waves to produce transient membrane permeability.

REFERENCES

1. Coleman, A.J., and Saunders, J.E., *Ultrasound Med. Biol.* **15**, 213-227 (1989).
2. Kodama, T., et al., *Ultrasound Med. Biol.* **24**, 1459-1466 (1998).
3. Kodama, T., et al., *Biophys. J.* **79**, 1821-1832 (2000).
4. Smondyrev, A.M., and Berkowitz M.L., *J. Comp. Chem.* **20**, 531-545 (1999).
5. Koshiyama, K., Master Thesis, Hokkaido University, (in Japanese), (2003).
6. Pearlman, D.A., et al., *Comp. Phys. Commun.* **91**, 1-41 (1995).
7. Humphrey, W., et al., J. Molec. Graphics **14**, 33-38 (1996).

e-mail contact: koshi@ring-me.eng.hokudai.ac.jp

British Journal of Cancer (2006) 95, 601–606

www.bjcancer.com

NK105, a paclitaxel-incorporating micellar nanoparticle, is a more potent radiosensitising agent compared to free paclitaxel

T Negishi[1], F Koizumi[1], H Uchino[2], J Kuroda[1], T Kawaguchi[3], S Naito[2] and Y Matsumura[*,1]

[1]Investigative Treatment Division, Research Center for Innovative Oncology, National Cancer Center Hospital East, 6-5-1 Kashiwanoha, Kashiwa, Chiba 277-8577, Japan; [2]Department of Urology, Graduate School of Medical Sciences, Kyushu University, 3-1-1 Maidashi, Higashi-ku, Fukuoka, Fukuoka 812-8582, Japan; [3]Department of Anatomy and Histology, Fukushima Medical University School of Medicine, 1-Hikariga-oka, Fukushima, Fukushima 960-1247, Japan

NK105 is a micellar nanoparticle formulation designed to enhance the delivery of paclitaxel (PTX) to solid tumours. It has been reported to exert antitumour activity *in vivo* and to have reduced neurotoxicity as compared to that of free PTX. The purpose of this study was to investigate the radiosensitising effect of NK105 in comparison with that of PTX. Lewis lung carcinoma (LLC)-bearing mice were administered a single intravenous (i.v.) injection of PTX or NK105; 24 h after the drug administration, a proportion of the mice received radiation to the tumour site or lung fields. Then, the antitumour activity and lung toxicity were evaluated. In one subset of mice, the tumours were excised and specimens were prepared for analysis of the cell cycle distribution by flow cytometry. Combined NK105 treatment with radiation yielded significant superior antitumour activity as compared to combined PTX treatment with radiation ($P=0.0277$). On the other hand, a histopathological study of lung sections revealed no significant difference in histopathological changes between mice treated with PTX and radiation and those treated with NK105 and radiation. Flow-cytometric analysis showed that NK105-treated LLC tumour cells showed more severe arrest at the G2/M phase as compared to PTX-treated tumour cells. The superior radiosensitising activity of NK105 was thus considered to be attributable to the more severe cell cycle arrest at the G2/M phase induced by NK105 as compared to that induced by free PTX. The present study results suggest that further clinical trials are warranted to determine the efficacy and feasibility of combined NK105 therapy with radiation.
British Journal of Cancer (2006) **95**, 601–606. doi:10.1038/sj.bjc.6603311 www.bjcancer.com
Published online 8 August 2006

Keywords: paclitaxel; NK105; radiosensitiser; polymer micelle; drug delivery system

Paclitaxel (PTX) has been demonstrated to be one of the most effective anticancer agents available at present (Carney, 1996; Khayat *et al*, 2000). Besides its antitumour activity, its ability to induce radiosensitisation has been reported both *in vitro* (Tishler *et al*, 1992; Choy *et al*, 1993; Lokeshwar *et al*, 1995; Rodriguez *et al*, 1995) and *in vivo* (Milas *et al*, 1994, 1995; Cividalli *et al*, 1998) this effect has been attributed to its effect of stabilising microtubules and inducing cell cycle arrest at the G2/M phase, the most radiosensitive phase of the cell cycle (Terasima and Tolmach, 1963; Sinclair and Morton, 1966). As several clinical studies have demonstrated the efficacy of PTX-based chemotherapy combined with radiotherapy, the combined modality is considered to be a potentially important treatment option for lung and breast cancer (Choy *et al*, 1998a, b, 2000; Dowell *et al*, 1999; Formenti *et al*, 2003; Kao *et al*, 2005).

The adverse effects of radiation, namely, lung toxicities in patients with breast or lung cancer treated by thoracic radiation, are of great concern, and may be dose limiting or even have a negative impact on the quality of life of the patients, even though radiation is an efficient treatment option. Lung toxicities often result in lung fibrosis, necessitating change of the treatment method and causing much distress or even death of the patients (Penney and Rubin, 1977; Early Breast Cancer Trialists' Collaborative Group, 2000; Lind *et al*, 2002). Some clinical trials actually reported an increased incidence of pneumonitis following combined PTX therapy with radiation in patients with breast or lung cancer (Taghian *et al*, 2001; Hanna *et al*, 2002; Chen and Okunieff, 2004).

Although widely used, PTX itself has several adverse effects, such as peripheral sensory neuropathy (Rowinsky *et al*, 1993; Rowinsky and Donehower, 1995), and its poor solubility in water is also associated with such effects as anaphylaxis and other severe hypersensitivity reactions attributable to Cremophor EL and ethanol, which are essential for solubilising PTX (Weiss *et al*, 1990; Rowinsky and Donehower, 1995). In order to overcome these problems, we prepared a new formulation, NK105, which is a PTX-incorporating polymeric micellar nanoparticle (85 nm in size) (Hamaguchi *et al*, 2005). NK105 is formed by facilitating the self-association of amphiphilic block copolymers constructed using polyethylene glycol (PEG) as the hydrophilic segment and modified polyaspartate as the hydrophobic segment in an aqueous medium. Owing to the PEG constituting the outer shell of the micelles, NK105 is soluble in water. In addition, PEG also confers a stealth property to the formulation, that allows the micellar drug preparation to be less avidly taken up by the reticuloendothelial

*Correspondence: Dr Y Matsumura; E-mail: yhmatsum@east.ncc.go.jp
Revised 5 June 2006; accepted 11 July 2006; published online 8 August 2006

system (RES) and to be retained in the circulation for a longer period of time (Klibanov *et al*, 1990, 1991; Allen, 1994; Gabizon *et al*, 1996). The prolonged circulation time and the ability of NK105 to extravasate through the leaky tumour vasculature (i.e., the EPR (enhanced permeability and retention) effect) causes accumulation of PTX in tumour tissues (Matsumura and Maeda, 1986; Maeda and Matsumura, 1989). We previously demonstrated that NK105 is associated with reduced neurotoxicity and also exerts more potent antitumour activity on human cancer xenograft, as compared to free PTX. In addition, because of its solubility in water, it is expected that the incidence of anaphylaxis and hypersensitivity reactions attributable to Cremophor EL and ethanol may also be reduced with NK105. A clinical trial of NK105 is now under way.

In this context, it is expected that the use of NK105 in place of PTX in combination with radiation may also yield superior results, because of the more potent antitumour activity of this drug as compared to that of free PTX. In this study, we evaluated the antitumour activity and severity of lung fibrosis induced by PTX and NK105 administered in combination with thoracic radiation, to examine whether combined NK105 chemotherapy with radiation would be an acceptable or useful treatment modality.

MATERIALS AND METHODS

Mice

Eight-week-old female C57BL/6J mice were purchased from Charles River Japan Inc. (Kanagawa, Japan). All the animal procedures were performed in compliance with the guidelines for the care and use of experimental animals, drawn up by the Committee for Animal Experimentation of the National Cancer Center; these guidelines meet the ethical standards required by law and also comply with the guidelines for the use of experimental animals in Japan.

PTX and NK105

Paclitaxel was purchased from Merican Corp. (Tokyo, Japan). NK105 is a PTX-incorporating 'core-shell-type' polymeric micellar nanoparticle formulation that was prepared by a previously reported procedure (Hamaguchi *et al*, 2005). Briefly, polymeric micellar particles were formed by facilitating the self-association of amphiphilic block copolymers in an aqueous medium. The polymer of NK105 was constructed using PEG as the hydrophilic segment and modified polyaspartate as the hydrophobic segment. The carboxylic groups of the polyaspartate block were modified by the esterification reaction with 4-phenyl-1-butanol, resulting in conversion of half of the groups to 4-phenyl-1-butanolate. Molecular weight of the polymers was determined to be approximately 2000 (PEG block: 12 000; moditied polyaspartate block: 8000).

Via the self-association process, PTX was incorporated into the inner core of the micelle system by physical entrapment through hydrophobic interactions between the drug and specifically well-designed block copolymers for PTX. NK105 was obtained as a freeze-dried formulation and contained ca.23% (WW^{-1}) of PTX. Finally, NK105, PTX-incorporating polymeric micellar nanoparticle formulation with a single and narrow size distribution, was obtained. The weight-average diameter of the nanoparticles was approximately 85 nm ranging from 20 to 430 nm.

Irradiation

The mice were anesthetised by intraperitoneal (i.p.) injection of nembutal (75 mg kg^{-1}) and placed on the stage for irradiation. The whole thorax or subcutaneous (s.c.) tumours of the thigh were irradiated using a Faxitron cabinet X-ray system model CP-160 by 100 kV X-rays from a linear accelerator, at a dose rate of 2 Gy min^{-1}. Totally 12 Gy was irradiated to each mouse. The whole body except irradiated parts, lung field or tumour lesion, were shielded with specially designed lead blocks.

Flow cytometry

At 24 h after the injection of PTX or NK105 into the Lewis lung carcinoma (LLC) tumour-bearing C57BL/6j mice, the tumours were excised, minced in PBS, and fixed in 70% ethanol at 4°C for 48 h. After being fixed, the tumours were digested with 0.04% pepsin (Sigma chemical co., St Louis, MO, USA) in 0.1 N HCl for 60 min at 37°C in a shaking bath for preparing single-nuclei suspensions. The nuclei were then centrifuged, washed twice with PBS, and stained with 40 $\mu g\,ml^{-1}$ of propidium iodide (Molecular Probes, OR, USA) in the presence of 100 $\mu g\,ml^{-1}$ RNase in 1 ml PBS for 30 min at 37°C. The stained nuclei were analysed with a B-D FACSCalibur (BD Biosciences, San Jose, CA, USA). The cell cycle distribution was analysed using the Modfit program (Verity Software House Inc., Topsham, ME, USA).

Evaluation of the antitumour activity

For this experiment, 3×10^6 LLC cells were inoculated s.c. into the right thighs of mice. The tumour volume was calculated using the formula, tumour volume (mm^3) $= a \times b^2/2$ (a = longest tumour diameter, b = shortest tumour diameter). When the tumour volume reached approximately 100 mm^3 on day 14 after the tumour inoculation, the mice were randomly allocated to test groups of about four or five mice each, and started the treatment on the same day. There were six test groups, as follows: untreated control, PTX treatment alone, NK105 treatment alone, radiation alone, combined PTX treatment with radiation, and combined with NK105 treatment with radiation.

In the groups receiving PTX or NK105, the mice were administered a single intravenous (i.v). injection of PTX or NK105 at the dose of 45 mg kg^{-1}; 24 h after the drugs were administered, the tumour sites of the mice in the groups scheduled to receive radiation were irradiated.

The antitumour activity of each treatment regimen was evaluated by measuring the tumour volume. Tumour volume and body weight was measured every 3 days.

Evaluation of lung toxicity

The severity of lung toxicity was evaluated histologically in the following test groups; untreated control ($n=6$), radiation treatment alone ($n=6$), combined PTX treatment with radiation ($n=9$), and combined NK105 treatment with radiation ($n=10$). Mice were administered a single i.v. injection of PTX or NK105 at the dose of 45 mg kg^{-1}; 24 h after the drugs were administered, the thorax of the mice in the groups scheduled to receive radiation was irradiated. All the mice were killed 36 weeks after the drug administration. At the time of the killing, the lungs were removed, and the right lungs were fixed in 10% buffered formalin for 24 h, then embedded in paraffin. The lungs were inflated at 20 cm water pressure by intratracheal infusion of 10% buffered formalin before fixation. Sections (5 μm- thick) were stained with haematoxylin and eosin (H&E) and observed under the light microscope. The severity of the pulmonary fibrosis was assessed based on Ashcroft's scoring system (Ashcroft *et al*, 1988). Briefly, all the fields of each lung section were scanned under a Leica microscope at a magnification of ×100, then each field was visually graded from 0 (normal lung) to 8 (total fibrotic obliteration of the field). The mean grades obtained for all of the fields was then calculated as the visual fibrotic score.

Immunohistochemistry

The lung sections were deparaffinised and rehydrated, then microwaved in 0.01 M sodium citrate buffer for 15 min at 90°C to retrieve epitopes, and cooled at room temperature. An endogenous peroxidase blocking solution of 3% hydrogen peroxide was applied for 20 min at room temperature. After blocking the nonspecific binding sites with 2% normal goat serum, the sections were incubated with rabbit anti-mouse collagen III immunoglobulin G (IgG) (Chemicon International, Temecula, CA, USA) overnight at 4°C. The sections were then washed with PBS, followed by the addition of biotin-conjugated goat anti-rabbit IgG (Vector Laboratories Inc., Burlingame, CA, USA) and incubation for 30 min at room temperature. The sections were then washed and incubated with horseradish-peroxidase-conjugated avidin–biotin complex (Vector Laboratories Inc., Burlingame, CA, USA) at room temperature for 30 min, in accordance with the manufacturer's instructions (Vector Laboratories Inc.). The immunoreactions were visualised using 3,3′-diaminobenzidine as the substrate and counterstaining with haematoxylin.

Statistical analysis

Date were expressed the mean ± s.d. Differences between the test groups were analysed by Student's *t*-test. We used Stat View (SAS Institute Inc.) statistical software. A value of $P<0.05$ was considered statistically significant.

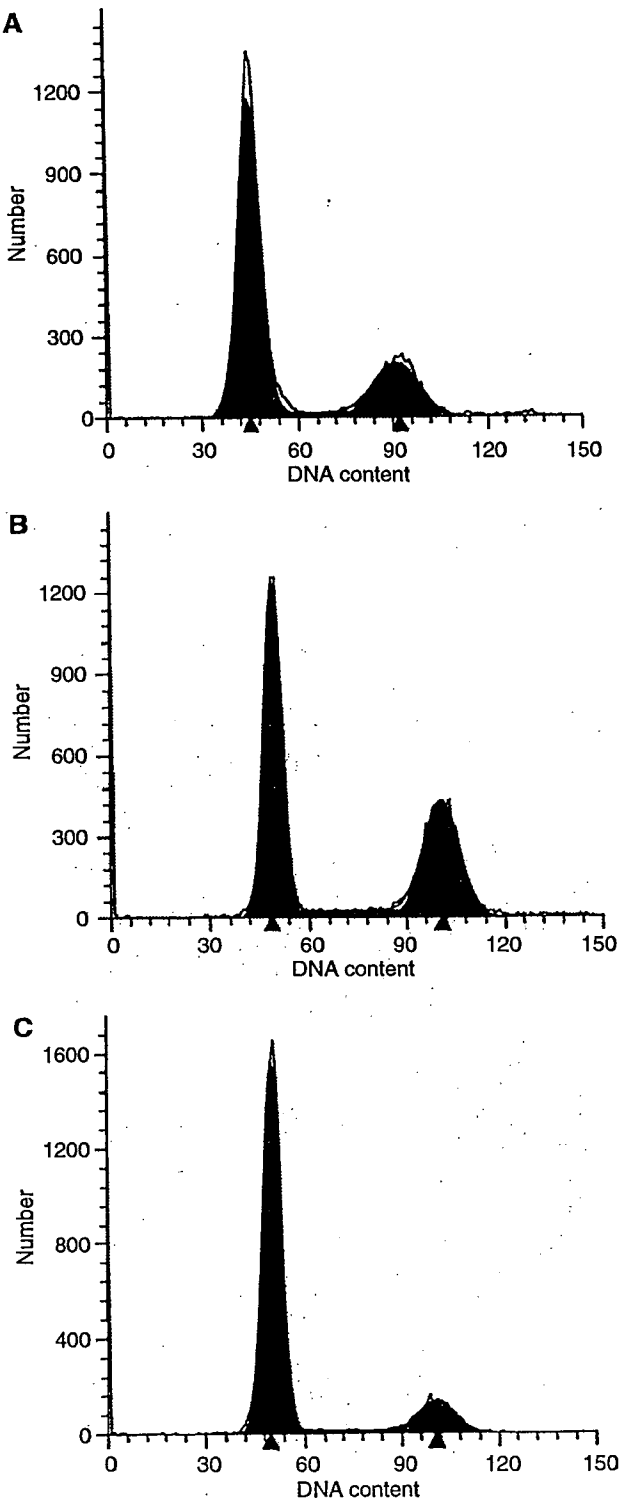

Figure 1 Cell cycle analysis. Cell cycle analysis of LLC tumour cells 24 h after PTX (**A**) or NK105 administration (**B**). Untreated control cells are shown in (**C**).

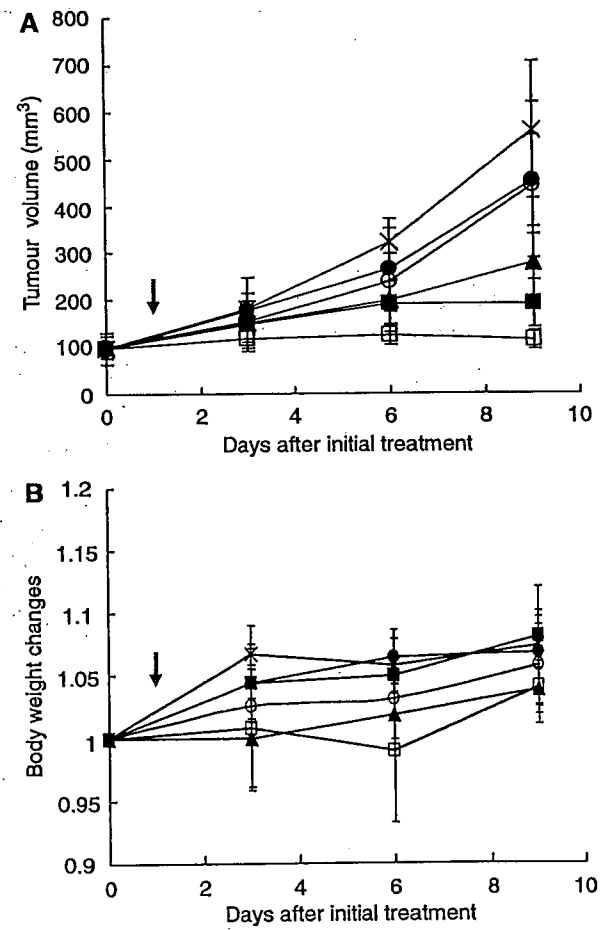

Figure 2 Antitumour activity. Changes in the LLC tumour growth rates in the mice. (**A**) Mice receiving TXL-alone (●), NK105-alone (○), combined treatment with PTX and radiation (■), and combined treatment with NK105 and radiation (□) were administered a single i.v. injection of PTX or NK105 at the dose 45 mg kg^{-1} on day 14 after the tumour inoculation (= on day 0 after the initial treatment). After 24 h the drugs were administered, the mice in the radiation-alone (△) and the combined-treatment groups were irradiated (arrow). Mice in the control group (×) were given no treatment. (**B**) Changes in the relative body weight. Data were derived from the same mice as those used in the present study.

RESULTS

Cell cycle analysis

At 24 h after the administration of PTX or NK105 to the LLC-tumour-bearing mice, severe cell cycle arrest at the G2/M phase was observed in the tumour cells treated with the drugs as compared with that in the control (no drug treatment) (Figure 1C). There was a tendency towards the NK105-treated LLC tumour cells (Figure 1B) showing more severe arrest at the G2/M phase than the PTX-treated cells (Figure 1A).

Antitumour activity

Decreased tumour growth rates of the LLC tumours were observed in the mice of the radiation alone, combined PTX with radiation, and combined NK105 with radiation groups. No antitumour activity was observed following treatment with either PTX or NK105 alone, because LLC is primarily a PTX-resistant tumour. Combined NK105 therapy with radiation yielded superior antitumour activity as compared to both radiation alone ($P=0.0047$) and combined PTX therapy with radiation ($P=0.0277$) on the day 9 after the treatment initiation (Figure 2A). No significant differences in body weight changes were noted among the groups tested (Figure 2B).

Lung toxicities

Histopathological examination of the lung sections of all the mice receiving radiation showed inflammatory cell infiltration, appearance of intra-alveolar macrophages, and destruction of the alveolar architecture. Major portions of the alveolar septa in the lung sections prepared from the irradiated mice showed slight thickening, although no massive structural destruction was observed (Figure 3A). On the other hand, the lung sections prepared from the control nonirradiated group showed no significant histopathological changes (Figure 3B). Ashcroft's fibrosis scores in the groups of mice that received radiation ranged from 0.975 to 1.426, with no significant differences among the groups. The score in the control group was nearly zero. In the groups receiving radiation, the severity of lung fibrosis differed significantly among the mice within the same groups, as did the Ashcroft's scores, that is, the s.d. of the Ashcroft's scores in the mice receiving radiation was very high (Figure 3C).

Type III collagen deposition

Immunohistochemical analysis of lung sections prepared from the mice receiving radiation revealed significant collagen deposition, especially in the subpleural regions, while that of lung sections prepared from the control group showed little collagen deposition. There were no significant differences among the different groups receiving radiation (Figure 3D).

DISCUSSION

It is well known that PTX enhances the radiosensitivity of tumour cells by inducing cell cycle arrest at the G2/M phase, the most radiosensitive phase of the cell cycle (Terasima and Tolmach, 1963;

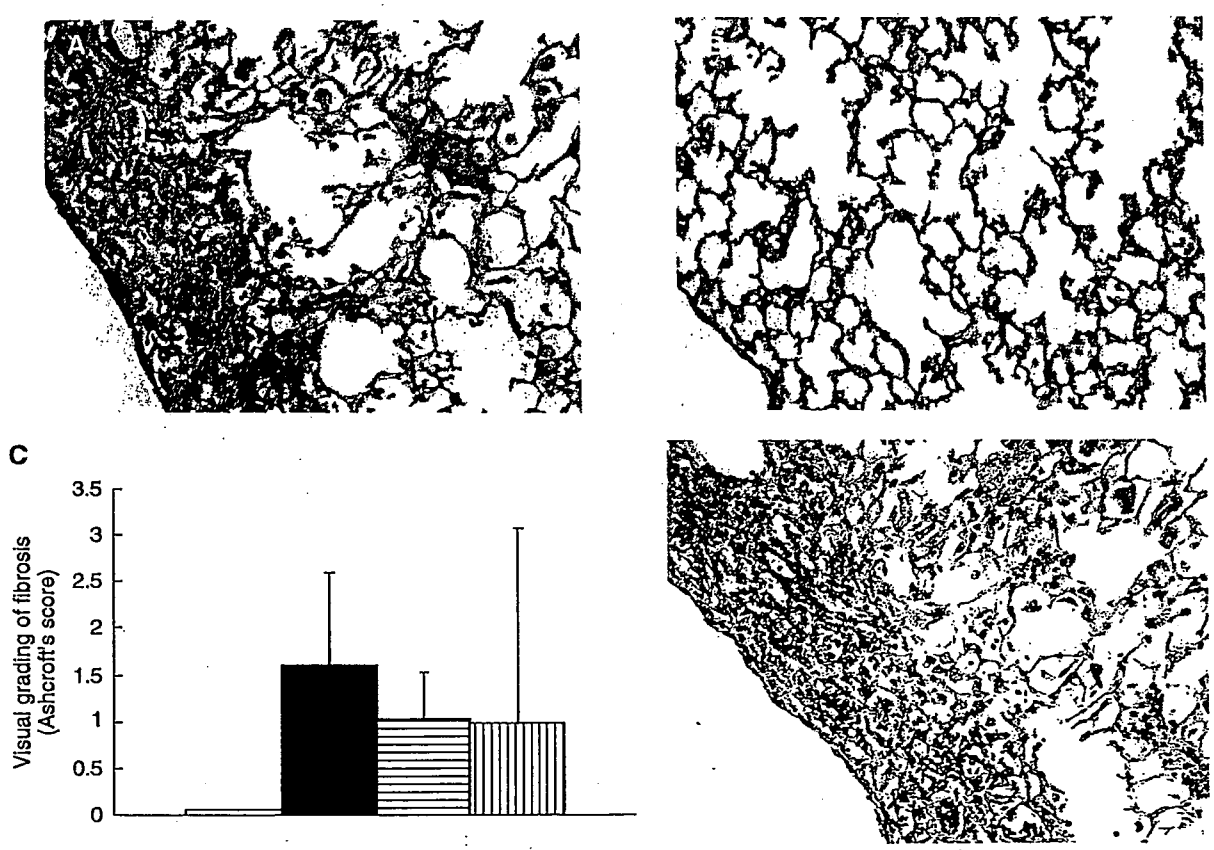

Figure 3 H&E staining of the lungs of C57BL/6J mice surviving 36 weeks after the thoracic radiation (**A**) and sham radiation (**B**). (**C**) Semiquantitative analyses to estimate the severity of pulmonary fibrosis in the mice receiving sham radiation (□), thoracic radiation alone (■), combined PTX with radiation (▤), and combined NK105 with radiation (▥). H&E- stained lung tissue sections were assessed to estimate the severity of pulmonary fibrosis by visual grading of fibrosis (Ashcroft's score). Collagen III staining of the irradiated lungs of mice (**D**).

Sinclair and Morton, 1966). Many reports have confirmed the radiosensitising effect of PTX in different cell lines (Tishler *et al*, 1992; Choy *et al*, 1993; Lokeshwar *et al*, 1995; Rodriguez *et al*, 1995), *in vivo* experiments (Milas *et al*, 1994, 1995; Cividalli *et al*, 1998), and in several clinical trials of combined PTX with radiation therapy according to different schedules (Dillman *et al*, 1990; Arriagada *et al*, 1991; Morton *et al*, 1991; Furuse *et al*, 1999; Sause *et al*, 2000; Chen *et al*, 2003). Chen *et al* (2003) examined the optimal timing of PTX treatment and irradiation in relation to the cell cycle, and recommended that radiation be given at least 5 h after PTX administration, because G2/M arrest of a lung cancer cell line was shown to start at 4 h after PTX treatment and to last for 44 h.

In our experimental model to evaluate the antitumour activity, the tumours were irradiated 24 h after a single i.v. injection of PTX or NK105. No significant increase in the antitumour activity as compared with that in the control (no treatment) was observed following a single i.v. injection of either PTX or NK105 at the dose of 45 mg kg^{-1}; LLC tumours are known to be primarily resistant to PTX. In fact, the IC_{50} of PTX against an LLC tumour cell line was shown to be 84.1 nM, which is about 10-fold higher than that of NK105 against various cancer cell lines tested in our previous work (Hamaguchi *et al*, 2005). Combined NK105 therapy with radiation yielded superior antitumour activity as compared with radiation alone or combined PTX therapy with radiation. This result suggests that NK105 has a more potent radiosensitising effect than PTX. In our study, there was a tendency towards NK105-treated LLC tumour cells showing more severe arrest at the G2/M phase as compared to PTX-treated cells at 24 h after the injection of the drugs, the timing of the radiation treatment, probably because NK105 allows a higher concentration of PTX to be maintained in the tumour than conventional PTX (Hamaguchi *et al*, 2005). We suppose that this is the reason why NK105 exerted more potent radiosensitising activity than PTX.

Next, we were concerned about the adverse effects of combined NK105 therapy with radiation. New micellar drugs are designed based on the idea that DDS can accumulate in the tumour selectively, while showing reduced distribution in normal tissues. We demonstrated that the incorporation of cisplatin into micelles significantly reduced the nephrotoxicity and neurotoxicity of cisplatin (Uchino *et al*, 2005). However, it was also shown that micelle- incorporated cisplatin caused transient liver dysfunction because it was trapped more avidly by the RES as compared to free cisplatin, even though the PEG of the outer shell of the micelle confers the so-called stealth effect.

In this study, our examination of the lung sections of mice treated with NK105 and radiation revealed that the histopathological changes such as inflammatory cell infiltration, appearance of intra-alveolar macrophages, and destruction of the alveolar architecture were induced by thoracic radiation and not by the accumulation of NK105 in the lung. There were no significant differences in the histopathological changes observed among the mice treated by NK105 and radiation and mice treated by radiation alone or PTX with radiation. The severity of lung fibrosis did not differ significantly among the test groups either. Although some clinical trials reported an increased incidence of pneumonitis and esophagitis following combined PTX therapy with radiation (Taghian *et al*, 2001; Hanna *et al*, 2002; Chen and Okunieff, 2004), others reported no influence on the incidence of such adverse effects (Ellerbroek *et al*, 2003; Yu *et al*, 2003). Several clinical trials and *in vivo* experiments have discussed the subject, however, no definitive conclusion has been arrived at (Mason *et al*, 1995; Choy *et al*, 1998; Yu *et al*, 2004; Kao *et al*, 2005). In our study, in regard to the incidence of esophagitis, there were no significant differences in the histopathological changes observed in the esophageal sections at one week after the treatment among the test groups (data not shown).

In conclusion, we demonstrated that combined NK105 chemotherapy with radiation exerts significant antitumour activity. Furthermore, the lung toxicity of this combined treatment modality was also acceptable as compared with that observed following radiation alone or combined PTX therapy with radiation. However, further studies are necessary to determine the effectiveness of NK105 in terms of its radiosensitising effect.

ACKNOWLEDGEMENTS

We thank Drs K Sugiyama and K Tsuchihara for their scientific advice and Mrs C Kanai and Mrs N Mie for their technical assistance. We are also grateful to Mrs K Shiina for her secretarial assistance. This work was supported by a Grant-in-Aid from the Ministry of Health, Labor and Welfare of Japan (Y Matsumura) and a Grant-in-Aid for Scientific Research on Priority Areas from the Ministry of Education, Culture, Sports, Science and Technology (Y Matsumura).

REFERENCES

Allen TM (1994) Long-circulating (sterically stabilized) liposomes for targeted drug delivery. *Trends Pharmacol Sci* 15: 215–220

Arriagada R, Le Chevalier T, Quoix E, Ruffie P, de Cremoux H, Douillard JY, Tarayre M, Pignon JP, Laplanche A (1991) ASTRO (American Society for Therapeutic Radiology and Oncology) plenary: Effect of chemotherapy on locally advanced non-small cell lung carcinoma: a randomized study of 353 patients. GETCB (Groupe d'Etude et Traitement des Cancers Bronchiques), FNCLCC (Federation Nationale des Centres de Lutte contre le Cancer) and the CEBI trialists. *Int J Radiat Oncol Biol Phys* 20: 1183–1190

Ashcroft T, Simpson JM, Timbrell V (1988) Simple method of estimating severity of pulmonary fibrosis on a numerical scale. *J Clin Pathol* 41: 467–470

Carney DN (1996) Chemotherapy in the management of patients with inoperable non-small cell lung cancer. *Semin Oncol* 23: 71–75

Chen Y, Okunieff P (2004) Radiation and third-generation chemotherapy. *Hematol Oncol Clin North Am* 18: 55–80

Chen Y, Pandya K, Keng PC, Johnstone D, Li J, Lee YJ, Smudzin T, Okunieff P (2003) Phase I/II clinical study of pulsed paclitaxel radiosensitization for thoracic malignancy: a therapeutic approach on the basis of preclinical research of human cancer cell lines. *Clin Cancer Res* 9: 969–975

Choy H, Akerley W, Safran H, Graziano S, Chung C, Williams T, Cole B, Kennedy T (1998a) Multiinstitutional phase II trial of paclitaxel, carboplatin, and concurrent radiation therapy for locally advanced non-small-cell lung cancer. *J Clin Oncol* 16: 3316–3322

Choy H, Devore III RF, Hande KR, Porter LL, Rosenblatt P, Yunus F, Schlabach L, Smith C, Shyr Y, Johnson DH (2000) A phase II study of paclitaxel, carboplatin, and hyperfractionated radiation therapy for locally advanced inoperable non-small-cell lung cancer (a Vanderbilt Cancer Center Affiliate Network Study). *Int J Radiat Oncol Biol Phys* 47: 931–937

Choy H, Rodriguez FF, Koester S, Hilsenbeck S, Von Hoff DD (1993) Investigation of taxol as a potential radiation sensitizer. *Cancer* 71: 3774–3778

Choy H, Safran H, Akerley W, Graziano SL, Bogart JA, Cole BF (1998b) Phase II trial of weekly paclitaxel and concurrent radiation therapy for locally advanced non-small cell lung cancer. *Clin Cancer Res* 4: 1931–1936

Cividalli A, Arcangeli G, Cruciani G, Livdi E, Cordelli E, Danesi DT (1998) Enhancement of radiation response by paclitaxel in mice according to different treatment schedules. *Int J Radiat Oncol Biol Phys* 40: 1163–1170

Dillman RO, Seagren SL, Propert KJ, Guerra J, Eaton WL, Perry MC, Carey RW, Frei III EF, Green MR (1990) A randomized trial of induction

chemotherapy plus high-dose radiation *vs* radiation alone in stage III non-small-cell lung cancer. *N Engl J Med* 323: 940–945

Dowell JE, Sinard R, Yardley DA, Aviles V, Machtay M, Weber RS, Weinstein GS, Chalian AA, Carbone DP, Rosenthal DI (1999) Seven-week continuous-infusion paclitaxel concurrent with radiation therapy for locally advanced non-small cell lung and head and neck cancers. *Semin Radiat Oncol* 9: 97–101

Early Breast Cancer Trialists' Collaborative Group (2000) Favourable and unfavourable effects on long-term survival of radiotherapy for early breast cancer: an overview of the randomised trials. Early Breast Cancer Trialists' Collaborative Group. *Lancet* 355: 1757–1770

Ellerbroek N, Martino S, Mautner B, Tao ML, Rose C, Botnick L (2003) Breast-conserving therapy with adjuvant paclitaxel and radiation therapy: feasibility of concurrent treatment. *Breast J* 9: 74–78

Formenti SC, Volm M, Skinner KA, Spicer D, Cohen D, Perez E, Bettini AC, Groshen S, Gee C, Florentine B, Press M, Danenberg P, Muggia F (2003) Preoperative twice-weekly paclitaxel with concurrent radiation therapy followed by surgery and postoperative doxorubicin-based chemotherapy in locally advanced breast cancer: a phase I/II trial. *J Clin Oncol* 21: 864–870

Furuse K, Fukuoka M, Kawahara M, Nishikawa H, Takada Y, Kudoh S, Katagami N, Ariyoshi Y (1999) Phase III study of concurrent *vs* sequential thoracic radiotherapy in combination with mitomycin, vindesine, and cisplatin in unresectable stage III non-small-cell lung cancer. *J Clin Oncol* 17: 2692–2699

Gabizon A, Chemla M, Tzemach D, Horowitz AT, Goren D (1996) Liposome longevity and stability in circulation: effects on the *in vivo* delivery to tumors and therapeutic efficacy of encapsulated anthracyclines. *J Drug Target* 3: 391–398

Hamaguchi T, Matsumura Y, Suzuki M, Shimizu K, Goda R, Nakamura I, Nakatomi I, Yokoyama M, Kataoka K, Kakizoe T (2005) NK105, a paclitaxel-incorporating micellar nanoparticle formulation, can extend *in vivo* antitumour activity and reduce the neurotoxicity of paclitaxel. *Br J Cancer* 92: 1240–1246

Hanna YM, Baglan KL, Stromberg JS, Vicini FA, A Decker D (2002) Acute and subacute toxicity associated with concurrent adjuvant radiation therapy and paclitaxel in primary breast cancer therapy. *Breast J* 8: 149–153

Kao J, Conzen SD, Jaskowiak NT, Song DH, Recant W, Singh R, Masters GA, Fleming GF, Heimann R (2005) Concomitant radiation therapy and paclitaxel for unresectable locally advanced breast cancer: results from two consecutive phase I/II trials. *Int J Radiat Oncol Biol Phys* 61: 1045–1053

Khayat D, Antoine EC, Coeffic D (2000) Taxol in the management of cancers of the breast and the ovary. *Cancer Invest* 18: 242–260

Klibanov AL, Maruyama K, Beckerleg AM, Torchilin VP, Huang L (1991) Activity of amphipathic poly(ethylene glycol) 5000 to prolong the circulation time of liposomes depends on the liposome size and is unfavorable for immunoliposome binding to target. *Biochim Biophys Acta* 1062: 142–148

Klibanov AL, Maruyama K, Torchilin VP, Huang L (1990) Amphipathic polyethyleneglycols effectively prolong the circulation time of liposomes. *FEBS Lett* 268: 235–237

Lind PA, Marks LB, Hardenbergh PH, Clough R, Fan M, Hollis D, Hernando ML, Lucas D, Piepgrass A, Prosnitz LR (2002) Technical factors associated with radiation pneumonitis after local +/– regional radiation therapy for breast cancer. *Int J Radiat Oncol Biol Phys* 52: 137–143

Lokeshwar BL, Ferrell SM, Block NL (1995) Enhancement of radiation response of prostatic carcinoma by taxol: therapeutic potential for late-stage malignancy. *Anticancer Res* 15: 93–98

Maeda H, Matsumura Y (1989) Tumoritropic and lymphotropic principles of macromolecular drugs. *Crit Rev Ther Drug Carrier Syst* 6: 193–210

Mason KA, Milas L, Peters LJ (1995) Effect of paclitaxel (taxol) alone and in combination with radiation on the gastrointestinal mucosa. *Int J Radiat Oncol Biol Phys* 32: 1381–1389

Matsumura Y, Maeda H (1986) A new concept for macromolecular therapeutics in cancer chemotherapy: mechanism of tumoritropic accumulation of proteins and the antitumor agent smancs. *Cancer Res* 46: 6387–6392

Milas L, Hunter NR, Mason KA, Kurdoglu B, Peters LJ (1994) Enhancement of tumour radioresponse of a murine mammary carcinoma by paclitaxel. *Cancer Res* 54: 3506–3510

Milas L, Hunter NR, Mason KA, Milross CG, Saito Y, Peters LJ (1995) Role of reoxygenation in induction of enhancement of tumour radioresponse by paclitaxel. *Cancer Res* 55: 3564–3568

Morton RF, Jett JR, McGinnis WL, Earle JD, Therneau TM, Krook JE, Elliott TE, Mailliard JA, Nelimark RA, Maksymiuk AW (1991) Thoracic radiation therapy alone compared with combined chemoradiotherapy for locally unresectable non-small cell lung cancer. A randomized, phase III trial. *Ann Intern Med* 115: 681–686

Penney DP, Rubin P (1977) Specific early fine structural changes in the lung irradiation. *Int J Radiat Oncol Biol Phys* 2: 1123–1132

Rodriguez M, Sevin BU, Perras J, Nguyen HN, Pham C, Steren AJ, Koechli OR, Averette HE (1995) Paclitaxel: a radiation sensitizer of human cervical cancer cells. *Gynecol Oncol* 57: 165–169

Rowinsky EK, Chaudhry V, Forastiere AA, Sartorius SE, Ettinger DS, Grochow LB, Lubejko BG, Cornblath DR, Donehower RC (1993) Phase I and pharmacologic study of paclitaxel and cisplatin with granulocyte colony-stimulating factor: neuromuscular toxicity is dose-limiting. *J Clin Oncol* 11: 2010–2020

Rowinsky EK, Donehower RC (1995) Paclitaxel (taxol). *N Engl J Med* 332: 1004–1014

Sause W, Kolesar P, Taylor SI, Johnson D, Livingston R, Komaki R, Emami B, Curran Jr W, Byhardt R, Dar AR, Turrisi III A (2000) Final results of phase III trial in regionally advanced unresectable non-small cell lung cancer: Radiation Therapy Oncology Group, Eastern Cooperative Oncology Group, and Southwest Oncology Group. *Chest* 117: 358–364

Sinclair WK, Morton RA (1966) X-ray sensitivity during the cell generation cycle of cultured Chinese hamster cells. *Radiat Res* 29: 450–474

Taghian AG, Assaad SI, Niemierko A, Kuter I, Younger J, Schoenthaler R, Roche M, Powell SN (2001) Risk of pneumonitis in breast cancer patients treated with radiation therapy and combination chemotherapy with paclitaxel. *J Natl Cancer Inst* 93: 1806–1811

Terasima T, Tolmach LJ (1963) X-ray sensitivity and DNA synthesis in synchronous populations of HeLa cells. *Science* 140: 490–492

Tishler RB, Geard CR, Hall EJ, Schiff PB (1992) Taxol sensitizes human astrocytoma cells to radiation. *Cancer Res* 52: 3495–3497

Uchino H, Matsumura Y, Negishi T, Koizumi F, Hayashi T, Honda T, Nishiyama N, Kataoka K, Naito S, Kakizoe T (2005) Cisplatin-incorporating polymeric micelles (NC-6004) can reduce nephrotoxicity and neurotoxicity of cisplatin in rats. *Br J Cancer* 93: 678–687

Weiss RB, Donehower RC, Wiernik PH, Ohnuma T, Gralla RJ, Trump DL, Baker Jr JR, Van Echo DA, Von Hoff DD, Leyland-Jones B (1990) Hypersensitivity reactions from taxol. *J Clin Oncol* 8: 1263–1268

Yu TK, Whitman GJ, Thames HD, Strom E, McNeese MD, Perkins GH, Schechter N, Kau S, Buzdar AU, Hortobagyi GN, Thomas E, Buchholz TA (2003) Clinically-relevant pneumonitis is not increased in breast cancer patients treated with sequential paclitaxel and radiation. *Int J Radiat Oncol Biol Phys* 57(2 Suppl): S127–S128

Yu TK, Whitman GJ, Thames HD, Buzdar AU, Strom EA, Perkins GH, Schechter NR, McNeese MD, Kau SW, Thomas ES, Hortobagyi GN, Buchholz TA (2004) Clinically relevant pneumonitis after sequential paclitaxel-based chemotherapy and radiotherapy in breast cancer patients. *J Natl Cancer Inst* 96: 1676–1681

Novel SN-38–Incorporating Polymeric Micelles, NK012, Eradicate Vascular Endothelial Growth Factor–Secreting Bulky Tumors

Fumiaki Koizumi,[1] Masayuki Kitagawa,[2] Takahito Negishi,[1] Takeshi Onda,[2] Shin-ichi Matsumoto,[2] Tetsuya Hamaguchi,[3] and Yasuhiro Matsumura[1]

[1]Investigative Treatment Division, Research Center for Innovative Oncology, National Cancer Center Hospital East, Kashiwa, Chiba, Japan; [2]Pharmaceutical Research Laboratories, Research and Development Group, Nippon Kayaku Co., Ltd, Kita-ku, Tokyo, Japan; and [3]Department of Medicine, National Cancer Center Hospital, Tyuo-ku, Tokyo, Japan

Abstract

7-Ethyl-10-hydroxy-camptothecin (SN-38), a biological active metabolite of irinotecan hydrochloride (CPT-11), has potent antitumor activity but has not been used clinically because it is a water-insoluble drug. For delivery by i.v. injection, we have successfully developed NK012, a SN-38-releasing nanodevice. The purpose of this study is to investigate the pharmacologic character of NK012 as an anticancer agent, especially in a vascular endothelial growth factor (VEGF)–secreting tumor model. The particle size of NK012 was ~20 nm with a narrow size distribution. NK012 exhibited a much higher cytotoxic effect against lung and colon cancer cell lines as compared with CPT-11. NK012 showed significantly potent antitumor activity against a human colorectal cancer HT-29 xenograft as compared with CPT-11. Enhanced and prolonged distribution of free SN-38 in the tumor was observed after the injection of NK012. NK012 also had significant antitumor activity against bulky SBC-3/Neo (1,533.1 ± 1,204.7 mm^3) and SBC-3/VEGF tumors (1,620.7 ± 834.0 mm^3) compared with CPT-11. Furthermore, NK012 eradicated bulky SBC-3/VEGF tumors in all mice but did not eradicate SBC-3/Neo tumors. In the drug distribution analysis, an increased accumulation of SN-38 in SBC-3/VEGF tumors was observed as compared with that in SBC-3/Neo tumors. NK012 markedly enhanced the antitumor activity of SN-38, especially in highly VEGF-secreting tumors, and could be a promising SN-38-based formulation. (Cancer Res 2006; 66(20): 10048-56)

Introduction

The antitumor plant alkaloid camptothecin (CPT) is a broad-spectrum anticancer agent that targets DNA topoisomerase I. Although CPT has shown promising antitumor activity *in vitro* and *in vivo* (1, 2), it has not been clinically used because of its low therapeutic efficacy and severe toxicity (3, 4). Among CPT analogues, irinotecan hydrochloride (CPT-11) has recently been shown to be active against colorectal, lung, and ovarian cancer (5–9). CPT-11 itself is a prodrug and is converted to 7-ethyl-10-hydroxy-CPT (SN-38), a biologically active metabolite of CPT-11, by carboxylesterases. SN-38 exhibits up to 1,000-fold more potent cytotoxic activity against various cancer cells *in vitro* than CPT-11 (10). Although CPT-11 is converted to SN-38 in the liver and tumor, the metabolic conversion rate is <10% of the original volume of CPT-11 (11, 12). In addition, the conversion of CPT-11 to SN-38 depends on the genetic interindividual variability of carboxylesterase activity (13). Thus, direct use of SN-38 might be of great advantage and attractive for cancer treatment. For the clinical use of SN-38, however, it is essential to develop a soluble form of water-insoluble SN-38. The progress of the manufacturing technology of "micellar nanoparticles" may make it possible to use SN-38 for *in vivo* experiments and further clinical use.

Passive targeting of drug delivery system is based on the pathophysiologic characteristics that are observed in many solid tumors: hypervascularity, irregular vascular architecture, potential for secretion of vascular permeability factors, and the absence of effective lymphatic drainage that prevents efficient clearance of macromolecules. These characteristics, unique to solid tumors, are believed to be the basis of the enhanced permeability and retention effect (14–17). Supramolecular structures, such as liposomes and polymeric micelles, are expected to increase the accumulation of drugs in tumor tissue through these pathophysiologic features. Polymeric micelle–based anticancer drugs have been developed in recent years (18–20), and some of them have been under evaluation for clinical trials (21–23). This carrier system can incorporate various kinds of drugs into the inner core by chemical conjugation or physical entrapment with relatively high stability, and the size can be controlled within the range of 20 to 100 nm in diameter. This range of diameters is too large to pass through normal vessel walls; therefore, the drug can be expected to reduce side effects due to a decrease in volume of distribution.

Angiogenesis is essential for the growth and metastasis of solid tumors (24). The clinical importance of angiogenesis in human tumors was shown by several reports indicating a positive relationship between the blood vessel density in the tumor mass and poor prognosis for survival in patients with various types of cancers (25–28). Furthermore, Natsume et al. (29) reported that the antitumor activities of anticancer agents, including *cis*-diammine-dichloroplatinum, vincristine, and docetaxel, were less active against vascular endothelial growth factor (VEGF)–secreting cells, SBC-3/VEGF, *in vivo* as compared with its mock transfectant (SBC-3/Neo), although the high vascularity should have been favorable for the drug delivery.

VEGF is also well known as a potent vascular permeability factor (30). The ability of supramolecular structures to accumulate in target tissue is based on the enhanced tumor angiogenesis and tumor vascular permeability that occur in solid tumors. Therefore, we hypothesized that a polymeric micelle–based drug carrier would increase its accumulation and deliver enhanced therapeutic efficacy in tumors that secrete higher levels of VEGF. In the present study, we present the superiority of NK012 over CPT-11 in a tumor model,

Requests for reprints: Yasuhiro Matsumura, Investigative Treatment Division, Research Center for Innovative Oncology, National Cancer Center Hospital East, 6-5-1 Kashiwanoha, Kashiwa, Chiba 277-8577, Japan. Phone: 81-4-7134-6857; Fax: 81-4-7134-6857; E-mail: yhmatsum@east.ncc.go.jp.

doi:10.1158/0008-5472.CAN-06-1605

especially in a VEGF-secreting tumor, and we illustrate the outstanding advantage of polymeric micelle–based drug carriers.

Materials and Methods

Drugs and Cells

SN-38 was synthesized by Nippon Kayaku Co., Ltd. (Tokyo, Japan). CPT-11 was purchased from Yakult Honsha Co., Ltd. (Tokyo, Japan). Human colon cancer cell lines WiDR, SW480, Lovo, and HT-29 and human non–small-cell lung cancer cell line A431 were purchased from American Type Culture Collection (Rockville, MD). Human small-cell lung cancer cell line SBC-3 and human non–small-cell lung cancer cell line PC-14 were kindly provided by Dr. I. Kimura (Okayama University, Okayama, Japan) and Dr. Y. Hayata (Tokyo Medical University, Tokyo, Japan), respectively. SBC-3 and PC-14 were maintained in RPMI 1640 supplemented with 10% fetal bovine serum (Cell Culture Technologies, Gaggenau-Hoerden, Germany), penicillin, streptomycin, and amphotericin B (100 units/mL, 100 μg/mL, and 25 μg/mL, respectively; Sigma, St. Louis, MO) in a humidified atmosphere of 5% CO_2 at 37°C. Other cell lines were maintained in DMEM (Nikken Bio Med. Lab., Kyoto, Japan) supplemented with 10% fetal bovine serum. SBC-3/Neo and SBC-3/VEGF were generated from SBC-3 cells that were transfected with BMG-Neo and BMG-Neo-VEGF as previously reported (29). The full-length sequence of human VEGF expressing 206 amino acids (31) was selected. SBC-3/VEGF cells express ~100 times more soluble VEGF than SBC-3/Neo and SBC-3 cells in the supernatant of cultured cells as shown by ELISA (29).

Preparation of an SN-38–Conjugated Poly(Ethylene Glycol)-Poly(Glutamic Acid) Block Copolymer for NK012 Construction

Poly(ethylene glycol)-poly(glutamic acid) block copolymer [PEG-PGlu(SN-38)] was synthesized as follows: A poly(ethylene glycol)-poly(glutamic acid) block copolymer [PEG-PGlu] was prepared according to the previously reported technique (32, 33). SN-38 was covalently introduced into the PGlu segment by the condensation reaction between the carboxylic acid on PGlu and the phenol on SN-38 with 1,3-diisopropylcarbodiimide and *N,N*-dimethylaminopyridine at 26°C. Consequently, the PGlu segment obtained sufficient hydrophobicity. Accordingly, NK012 was constructed with self-assembling PEG-PGlu(SN-38) amphiphilic block copolymers in an aqueous milieu.

Determination of the Size Distribution of NK012 and Drug Release Behavior of SN-38 from NK012

The size distribution of NK012 was measured with the dynamic light scattering method at 25°C using a Particle Sizer NICOMP 380ZLS (Particle Sizing Systems, Santa Barbara, CA). The release behavior of SN-38 from NK012 was investigated *in vitro* at 20°C or 37°C in PBS (pH 7.3) or 5% glucose solution (pH 4.6). The concentration was 0.1 mg/mL. The amount of SN-38 released from NK012 was estimated by UV measurement at 265 nm.

In vitro Growth Inhibition Assay

The growth inhibitory effects of NK012, SN-38, and CPT-11 were examined with a 3-(4,5-dimethylthiazol-2-yl)-2,5-diphenyltetrazolium bromide (MTT) assay. One hundred eighty microliters of an exponentially growing cell suspension (6×10^3/mL-12×10^3/mL) were seeded into a 96-well microtiter plate, and 20 μL of various concentrations of each drug were added. After incubation for 72 hours at 37°C, 20 μL of MTT solution (5 mg/mL in PBS) were added to each well and the plates were incubated for an additional 4 hours at 37°C. After centrifuging the plates at 200 × *g* for 5 minutes, the medium was aspirated from each well, and 180 μL of DMSO were added to each well to dissolve the formazan. The growth inhibitory effect of each drug was assessed spectrophotometrically (SpectraMax 190, Molecular Devices Corp., Sunnyvale, CA).

In vivo Growth Inhibition Assay

The animal experimental protocols were approved by the Committee for Ethics of Animal Experimentation and the experiments were conducted in accordance with the Guidelines for Animal Experiments in the National Cancer Center or Nippon Kayaku.

Experiment 1. Female BALB/c nude mice, 7 weeks old, were purchased from CLEA Japan (Tokyo, Japan). Human colorectal cancer HT-29 cells were grown as s.c. tumor in the flank of the mice. The tumors were excised from the mice and fragments were inoculated s.c. in the mouse flank. When the tumor volume reached 70 to 170 mm^3, mice were randomly divided into test groups consisting of six mice per group (day 0). Drugs were administered on days 0, 4, and 8 by i.v. injection into the tail vein. NK012 was given at doses of 30 (maximum tolerated dose), 15, and 7.5 mg/kg/d. The reference drug, CPT-11, was given at the maximum tolerated dose, 66.7 mg/kg/d, in the optimal schedule reported (34). The length (a) and width (b) of the tumor mass were measured twice a week, and the tumor volume (TV) was calculated as follows: $TV = (a \times b^2) / 2$. Relative tumor volumes at day n were calculated according to the following formula: $RTV = TV_n / TV_0$, where TV_n is the tumor volume at day n, and TV_0 is the tumor volume at day 0. Differences in relative tumor sizes between the treatment groups at day 21 were analyzed with an unpaired t test.

Experiment 2. As a hypervascular tumor model, we used SBC-3/VEGF cells. SBC-3/Neo or SBC-3/VEGF cells (10^7) were s.c. injected into the back of mice. NK012 or CPT-11 was administered when the mean tumor volumes ($n = 4$) reached a massive size of 1,500 mm^3, which gave tumors almost 1.5 cm in length. It took ~65 days for SBC-3/Neo and 20 days for SBC-3/VEGF to reach the tumor volume of 1,500 mm^3 from the day of inoculation. NK012 at a dose of 10 or 20 mg/kg/d and CPT-11 at a dose of 15 or 30 mg/kg/d were administered i.v. on days 0, 4, and 8. Differences in tumor sizes between the treatment groups and control group at day 14 were analyzed with an unpaired t test.

Histologic and Immunohistochemical Analysis

Histologic sections were taken from SBC-3/Neo and SBC-3/VEGF tumor tissues when the volumes reached 1,500 mm^3. After extirpation, tissues were fixed with 3.9% formalin in PBS (pH 7.4), and the subsequent preparations and H&E staining were done by Tokyo Histopathologic Laboratory Co., Ltd. (Tokyo, Japan). For detection of tumor blood vessels, polyclonal anti–von Willebrand factor antibody (Dako, Glostrup, Denmark) was used.

Assay for SN-38 and CPT-11 in Plasma and Tissues

Female BALB/c nude mice bearing HT-29 (as mentioned in experiment 1; $n = 3$) were used for the analysis of the biodistribution of NK012 and CPT-11. NK012 (30 mg/kg) or CPT-11 (66.7 mg/kg) was administered i.v. to the mice. Under anesthesia, blood and tumor samples were taken at 5 minutes, 1, 6, 24, 48, 72, and 168 hours after administration of NK012 and at 5 minutes, 1, 3, 6, and 24 hours after administration of CPT-11. The blood samples were collected in microtubes and immediately centrifuged at 1,600 × *g* for 15 minutes. The plasma and tumor samples were stored at −80°C until analysis.

For the biodistribution study in hypervascular tumors (experiment 2), female BALB/c nude mice ($n = 3$) bearing 1,500-mm^3 massive SBC-3/Neo and SBC-3/VEGF tumors were used. NK012 (20 mg/kg) and CPT-11 (30 mg/kg) were administered on day 0. The mice were sacrificed at 1, 6, 24, and 72 hours (day 3) after administration. The tumor, liver, spleen, upper small intestine, lung, and blood were taken and stored at −80°C until analysis.

Preparation of the free SN-38 (polymer-unbound SN-38) and CPT-11. Tumor samples were homogenized on ice using a Digital homogenizer (Iuchi, Osaka, Japan) and suspended in the mixture of 100 mmol/L glycine-HCl buffer (pH 3)/methanol (1:1, v/v) at a concentration of 5% w/w. The concentrations of free SN-38 and CPT-11 in the plasma and tumor from aliquots of the homogenates (100 μL) and plasma (50 μL) were determined by high-performance liquid chromatography. For free SN-38 (polymer-unbound SN-38) and CPT-11, proteins were precipitated with an ice-cold mixture of methanol/H_2O/$HClO_4$ (50:45:5, v/v/v) containing CPT as an internal standard. The sample was vortexed for 10 seconds, filtered through a MultiScreen Solvinert (Millipore Corp., Bedford, MA), and analyzed.